

Article

Multidisciplinary Approaches for Assessing a High Temperature Borehole Thermal Energy Storage Facility at Linköping, Sweden

Max Hesselbrandt ¹, Mikael Erlström ^{2,3} , Daniel Sopher ⁴ and Jose Acuna ^{1,5,*} 

¹ Bengt Dahlgren AB, Hammarby Allé 47, SE-120 30 Stockholm, Sweden; max.hesselbrandt@bengtdahlgren.se

² Geological Survey of Sweden, Kiliansgatan 10, SE-223 50 Lund, Sweden; mikael.erlstrom@sgu.se

³ Department of Geology, Faculty of Science, Lund University, Sölvegatan 12, SE-223 62 Lund, Sweden

⁴ Geological Survey of Sweden, Box 670, SE-751 28 Uppsala, Sweden; daniel.sopher@sgu.se

⁵ Department of Geoscience and Petroleum, Faculty of Engineering, Norwegian University of Science and Technology, S.P. Andersens veg 15a, 7031 Trondheim, Norway

* Correspondence: jose.acuna@ntnu.no; Tel.: +46-762-320-008

Abstract: Assessing the optimal placement and design of a large-scale high temperature energy storage system in crystalline bedrock is a challenging task. This study applies and evaluates various methods and strategies for pre-site investigation for a potential high temperature borehole thermal energy storage (HT-BTES) system at Linköping in Sweden. The storage is required to shift approximately 70 GWh of excess heat generated from a waste incineration plant during the summer to the winter season. Ideally, the site for the HT-BTES system should be able to accommodate up to 1400 wells to 300 m depth. The presence of major fracture zones, high groundwater flow, anisotropic thermal properties, and thick Quaternary overburden are all factors that play an important role in the performance of an HT-BTES system. Inadequate input data to the modeling and design increases the risk of unsatisfactory performance, unwanted thermal impact on the surroundings, and suboptimal placement of the HT-BTES system, especially in a complex crystalline bedrock setting. Hence, it is crucial that the subsurface geological conditions and associated thermal properties are suitably characterized as part of pre-investigation work. In this study, we utilize a range of methods for pre-site investigation in the greater Distorp area, in the vicinity of Linköping. Ground geophysical methods, including magnetic and Very Low-Frequency (VLF) measurements, are collected across the study area together with outcrop observations and lab analysis on rock samples. Borehole investigations are conducted, including Thermal Response Test (TRT) and Distributed Thermal Response Test (DTRT) measurements, as well as geophysical wireline logging. Drone-based photogrammetry is also applied to characterize the fracture distribution and orientation in outcrops. In the case of the Distorp site, these methods have proven to give useful information to optimize the placement of the HT-BTES system and to inform design and modeling work. Furthermore, many of the methods applied in the study have proven to require only a fraction of the resources required to drill a single well, and hence, can be considered relatively efficient.

Keywords: methodology; crystalline bedrock; energy storage; boreholes; logging; thermal properties; magnetic measurements; VLF; drone photogrammetry



Citation: Hesselbrandt, M.; Erlström, M.; Sopher, D.; Acuna, J. Multidisciplinary Approaches for Assessing a High Temperature Borehole Thermal Energy Storage Facility at Linköping, Sweden. *Energies* **2021**, *14*, 4379. <https://doi.org/10.3390/en14144379>

Academic Editors: Renato Somma and Daniela Blessent

Received: 20 February 2021

Accepted: 7 July 2021

Published: 20 July 2021

Publisher's Note: MDPI stays neutral with regard to jurisdictional claims in published maps and institutional affiliations.



Copyright: © 2021 by the authors. Licensee MDPI, Basel, Switzerland. This article is an open access article distributed under the terms and conditions of the Creative Commons Attribution (CC BY) license (<https://creativecommons.org/licenses/by/4.0/>).

1. Introduction

Waste heat is an inevitable byproduct generated during the process of energy conversion. An estimated 50% of the global primary energy production is dissipated as exhaust losses, with the main portion being relatively low-grade heat at temperatures below 100 °C [1]. Thermal energy storage (TES) systems provide a possibility to harness this wasted heat and correct temporal phase differences between heat supply and demand in single buildings, as well as in large-scale district heating systems. One such system

is borehole thermal energy storage (BTES), which uses the ground as a storage medium together with shallow vertical borehole heat exchangers (BHE). A heat transfer fluid is circulated through the BHE network, which exchanges heat with the surrounding subsurface. These systems have been used successfully for a couple of decades for storing and recovering heat, as well as cold, in residential and commercial buildings [2]. Typically, these systems operate at temperatures that are relatively close to the undisturbed or natural temperature of the subsurface. Only a few high temperature BTES (HT-BTES) systems, which operate at temperatures significantly above ambient conditions, have been built [3]. However, due to social, environmental, and economic drivers, interest in using HT-BTES systems for storing large amounts of waste heat at high temperatures (50 to 100 °C) is presently increasing. In such systems, the size, performance, and economic feasibility rely strongly on the capacity of the subsurface to store and transport heat.

This study investigates the potential to implement an HT-BTES system in the city of Linköping, Sweden. The average yearly temperature in Linköping is 7.4 °C, where the monthly average temperatures range between −1.9 °C in the winter and 17.9 °C in the summer [4]. The number of yearly heating degree days (HDD) for the period 2011–2016 in the Linköping area is 3602, which is significantly higher in comparison to Central Europe, where the typical HDD value is less than 2500 [5]. The relatively high HDD value results in a great need for heating of housing in Linköping, which is typical for urban areas in the Nordic countries. Presently, the heating demand in Linköping is met mainly by a district heating system powered primarily by energy from a waste incineration plant. This plant has a heat capacity of 510 GWh, which corresponds to the heating required for about 25,000 houses [6]. Today most of the excess heat produced during electricity generation in the summertime cannot be utilized, and is, thus, wasted. During the wintertime, fossil-fueled plants are used to cover the peak heating demand.

Presently, Tekniska Verken in Linköping AB (a large energy company in Sweden) is assessing the option to store excess heat (about 70 GWh) from their combined heat and power (CHP) operation in an HT-BTES during the summer period and to utilize it during the peak-load periods in the winter. Such a system could increase the flexibility and efficiency of the energy system. In addition, it could make it possible to phase out the fossil-fueled plants, used to generate additional heat during the winter. If the geological, social, and techno-economical prerequisites are met for the site, it could become one of the largest HT-BTES systems in the world. Earlier modeling work of a potential HT-BTES system in Linköping is described in [7], where the Precambrian crystalline bedrock is considered as the storage medium. According to that study, a heat pump-supported HT-BTES system consisting of 1300 to 1500 BHEs with 300 m depth shows a potential to store and extract up to c. 90 GWh annually. In this study, a system with up to 1400 BHEs, borehole depth of about 300 m, and well separation of five meters is assumed.

The design of an HT-BTES plant is a complex and challenging endeavor that involves social, environmental, techno-economical, and practical aspects. The design work involves calculations of the energy efficiency, as well as energy and exergy balance. Hence, as input to this process, it is important to understand the thermal properties of the bedrock, the amount of fracturing and its orientation, groundwater conditions and water chemistry, as well as the thermal impact on the system design [8].

With regards to the potential storage site, there are several factors that would be desirable for the efficient operation of a potential HT-BTES system. Since the TES solution is based on the storage of sensible heat, a high volumetric heat capacity of the bedrock is desirable as this will ultimately lead to a higher thermal energy storage potential for the site. Furthermore, high thermal conductivity of the subsurface is beneficial, since it promotes rapid heat transfer within the storage, and will, thus, contribute to the higher short-term performance of the BHEs [2]. It is, however, important to note that high rates of conductive heat transfer also promote heat losses to the surrounding subsurface, and consequently reduce the long-term performance of the storage [9,10]. In addition, HT-BTES systems in fractured rock can be subject to substantial advective losses in the presence of groundwater

flow [11]. Extensive fracturing in some cases can also complicate drilling and lead to well integrity problems. Hence, site conditions characterized by low-permeability bedrock combined with low hydraulic gradients are also desirable.

Often, there is uncertainty as to the best available methodology for assessing the suitability of a potential site for a large-scale HT-BTES. Historically, closed-loop shallow geothermal energy system development has primarily been driven as a subset of heating, ventilation, and air-conditioning (HVAC) research, focusing on energy performance, heat pump technology, and the design of mechanical devices, etc. As a result, the characteristics of the geological and hydrogeological environment surrounding the boreholes have typically been of lesser concern [12,13]. Presently, standard assumptions about bedrock composition, overburden thickness, and thermal properties are often made based on regional data from geological maps combined with thermal response test data from one or a few scattered test boreholes. Furthermore, most existing design methodologies assume the homogeneous rock mass [14]. These general assumptions are often enough for the design of smaller and low temperature BTES. However, to optimally position, as well as better prognose the performance and reliability of large-scale high temperature systems that can hypothetically be connected to district heating production, better characterization of the bedrock storage medium is required. Concerns about the environmental impact of BTES systems are also increasing as subsurface resources are more exploited in parallel with population growth and urbanization. As pointed out by [13], sustainable BTES development requires a profound understanding of the full range of concerns associated with the technical, geological, and hydrogeological aspects of the ground-coupled system and its interaction with subsurface processes. This could be achieved by deeper integration between mechanical and geosciences disciplines to use their combined expertise in the fields involved.

Immediately north of the city of Linköping, Sweden, a relatively large area (about 2 km²), referred to as the Distorp site, has been identified within which a potential HT-BTES system could be situated. Based on the previously available geological information, both the type of bedrock and distribution of fractures is expected to vary significantly within the area. Heterogeneity within a storage medium, which has not been adequately characterized, is known to be a factor that can reduce the accuracy of modeling and design efforts. For example, [15] shows that a better understanding of subsurface heterogeneity in the modeling of BTES systems can reduce uncertainty in energy balance calculations. Similarly, work by [11,16] showed that groundwater movement can also significantly impact the performance of a BTES facility. Therefore, to place investigation boreholes optimally and efficiently and subsequently locate and accurately model the performance of a full-scale HT-BTES system, improved knowledge of the subsurface geology across the study area is required.

In this study, a multidisciplinary approach is adopted to investigate the geology of the Distorp site and to provide information to help optimize future investigation work, as well as the design of a potential HT-BTES system. Surface-based geological and geophysical measurements, not typically included in pre-investigation surveys for BTES systems, are combined with more conventional, as well as state-of-the-art measurements in several boreholes. Finally, some of the merits and limitations of the different methods applied in this study are discussed in the context of pre-site investigation for an HT-BTES system. Hence, the aims for the study are: (1) To provide a case study of multidisciplinary pre-investigation work at the Distorp site to exemplify how this information can be used to reduce risk in the placement and planning of an HT-BTES system; (2) to test and evaluate the applicability of many different field methods, not typically applied in pre-investigation work for BTES systems, to guide as to what information can and should be collected during field study and design of HT-BTES.

2. Geological Setting at Distorp, Linköping

The site to be addressed in this study has previously been identified as a potential area for constructing a high temperature BTES. The site lies within a small region of farmland called Distorp, located a few kilometers north of Linköping. The terrain in Distorp can be characterized as a low-lying hilly landscape, which is like the terrain of much of the surrounding region.

The bedrock in Distorp is typically draped by less than ten meters of Quaternary deposits, consisting of clay, silty clay, and clayey till. The terrain altitude in the site area varies between 38 and 47 m above mean sea level. Relatively thick Quaternary clay-dominated deposits are mainly found in the lower parts of the terrain, while thin deposits of till are associated with topographic highs. In several places, the Quaternary deposits are absent, and the underlying bedrock is exposed. These bedrock outcrops often exhibit smooth and rounded geometries, due to glacial erosion, and can be observed at several locations within the Distorp site and surrounding area. In addition, the main N–S direction of the ice during the last glaciation has created a corresponding lineation of the landscape. The terrain also clearly portrays the presence of regional NW–SE- and NNW–SSE-oriented fracture and deformation zones that have been further contoured by Quaternary glacial erosion and deposition. These zones are related to a structural belt of folded and metamorphosed rocks affected by the Svecokarelian orogen (c. 1.86 Ga) [17].

Overall, the bedrock is strongly affected by ductile deformation and amphibolite to locally granulite facies metamorphism. Metabasaltic rocks of amphibolite and gabbro, as well as diorite, are found within domains of variably gneissic and granitoid intrusive rocks. Besides these, a series of post-Svecokarelian (c. 1.85–1.65 Ga) variably porphyric, granulitic, and gneissic granites intrude the previous rock suites. Within the Linköping area there are also subordinate occurrences of Svecofennian supracrustal (c. 1.91–1.86 Ga) metamorphosed felsic rhyolitic volcanoclastics [18]. Based on modal data presented in the description of the bedrock map of Linköping NE [19], the average SiO₂ content (which largely influences the thermal conductivity of the rock) is 68–75% for the gneissic and granitoid rocks, and 45–52% for the metabasaltic rocks.

The predominance of NW–SE-oriented structures (fractures, faults, and deformation zones) is related to the Loftahammar–Linköping regional deformation zone (LLDZ) marking the boundary between the Bergslagen (to the NE) and Småland (to the SW) lithotectonic units [17]. This 7–10 km wide zone includes, besides a break in the topography, a series of ductile and brittle deformation zones. The LLDZ is clearly visible in the Geological Survey of Sweden's (SGU) geophysical data, as a broad NW–SE-oriented region with anomalously low values in the magnetic data. In the gravity data it appears as a region with a distinct N–S-oriented gradient with higher gravity values occurring in the north [18]. Since the Distorp site is located within the LLDZ, adjacent to the N–E boundary, several NE–SW-oriented lineaments parallel to the main orientation of the zone are expected (Figure 1).

The Distorp site also lies in the periphery of an area to the west with Lower Paleozoic platform cover strata [20]. As the outer eastern part of this area is located immediately north of the site area (Figure 1), scattered and thin deposits of Cambrian sandstone can be expected on top of the Precambrian bedrock.

The groundwater resources in the area are mainly associated with the bedrock, since the overburden is dominated by thin fine-grained deposits with low transmissivity and storage capacity. Data from the publicly available well information database at the Geological Survey of Sweden show that wells drilled in the granite-dominated areas give capacities between 1000 and 2000 L/h, while wells in metabasite and gabbroid bedrock areas show capacities <600 L/h [21].

It is clear from the regional geological information that variations in the lithology and level of deformation of the crystalline basement are expected to occur across the area of the Distorp site. Furthermore, in some areas, the crystalline basement can be overlain by variable, albeit relatively thin sequences of Cambrian strata or Quaternary sediments.

Hence, it is important to consider these anisotropic bedrock conditions when performing future appraisal investigations and during the design of the energy storage.

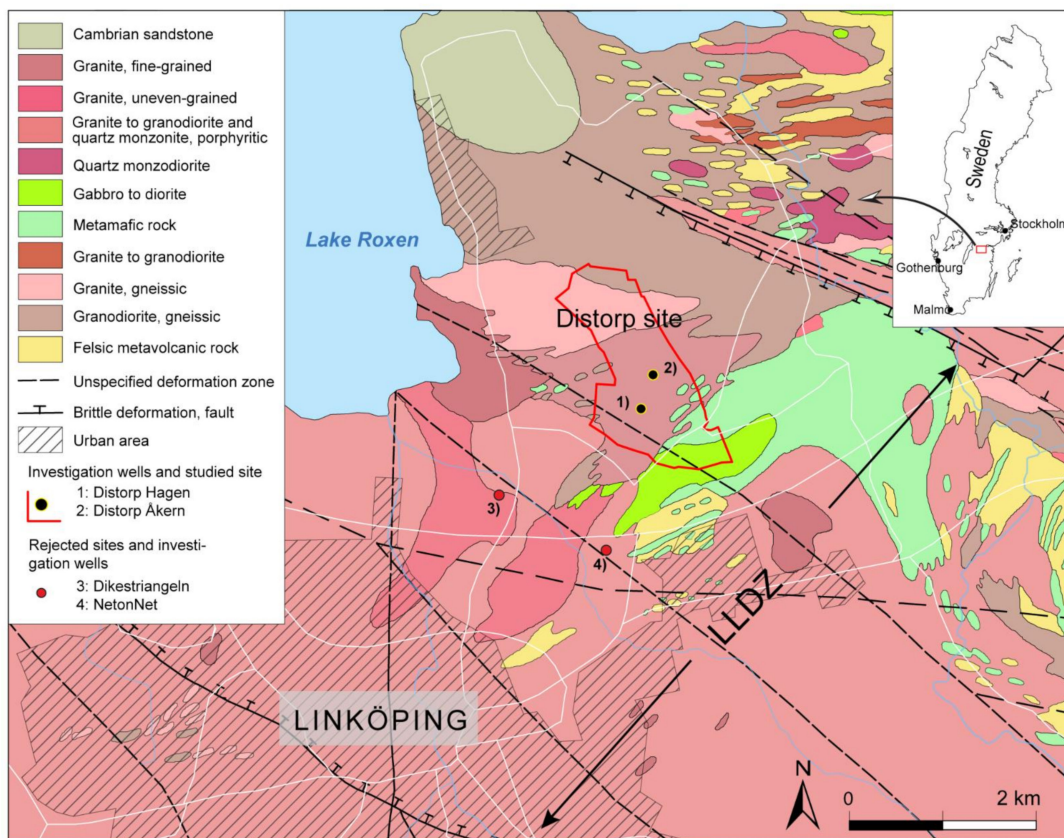


Figure 1. Bedrock geological map of the Distorp site (red frame) and surroundings extracted from the Geological Survey of Sweden’s bedrock database. LLDZ, Loftahammar–Linköping deformation zone. Map modified with permission after [18]. © Sveriges geologiska undersökning.

3. Methods

The primary aim for pre-investigation in any HT-BTES project is to evaluate the geological and thermal conditions of the subsurface with respect to their suitability for the potential development of an HT-BTES facility. In this study, we discuss and present exhaustive pre-investigation work which has been done at the Distorp site, Linköping.

Prior to selecting the Distorp site for more detailed investigations in this study, four different locations were selected as preliminary sites. The choice of these four sites was essentially based on the availability of accessible land areas at a suitable distance from Tekniska Verken in Linköping AB’s waste incineration plant Gärstadverket, i.e., the heat waste source for the possible HT-BTES. This first phase of the investigations was carried out in 2017 and started with the completion of one 300 m deep percussion borehole (115 mm Ø) in each of the four locations, i.e., Dikesträngeln, NetonNet, Distorp Åkern, and Distorp Hagen (Figure 1). The work included collecting samples of drill cuttings, measuring drilling time per drilling rod, and monitoring groundwater levels. Furthermore, temperature measurements, hydraulic capacity tests, thermal response tests (TRT), and distributed thermal response tests (DTRT) were also performed [22]. Two of the four preliminary locations were disregarded, due to the presence of relatively thick overburden, the occurrence of biogenic gas in the soil, and comparatively low thermal conductivity. The remaining two sites, referred to as Distorp Åkern and Distorp Hagen, were subsequently merged into one larger prospect site for further investigations in this study, i.e., the ca 2 km² large Distorp site (Figure 1).

In the Distorp site, three investigation wells have been established [22], including the two 300 m deep boreholes drilled during the first investigation phase in 2017 (Distorp Hagen and Distorp Åkern). In 2018, an additional investigation well (89 mm Ø) was drilled adjacent to the Distorp Hagen well using a water-driven down-the-hole (DTH) system to a depth of approximately 240 m [23]. These two wells were selected for conducting field experiments intended for investigating and applying permeation grouting techniques as a means of reducing fluid loss in open-loop BHEs. With a surface distance of only around 2.5 m between the Distorp Hagen wells, the well configuration represents typical conditions in BTES construction where very dense drilling grids are common.

Figure 2 presents the various steps of the multidisciplinary investigations and methodologies used at the Distorp site as part of this study. Figure 2 also presents the associated information or data obtained from applying these methods, which are relevant to evaluating the site and input to the HT-BTES design work.

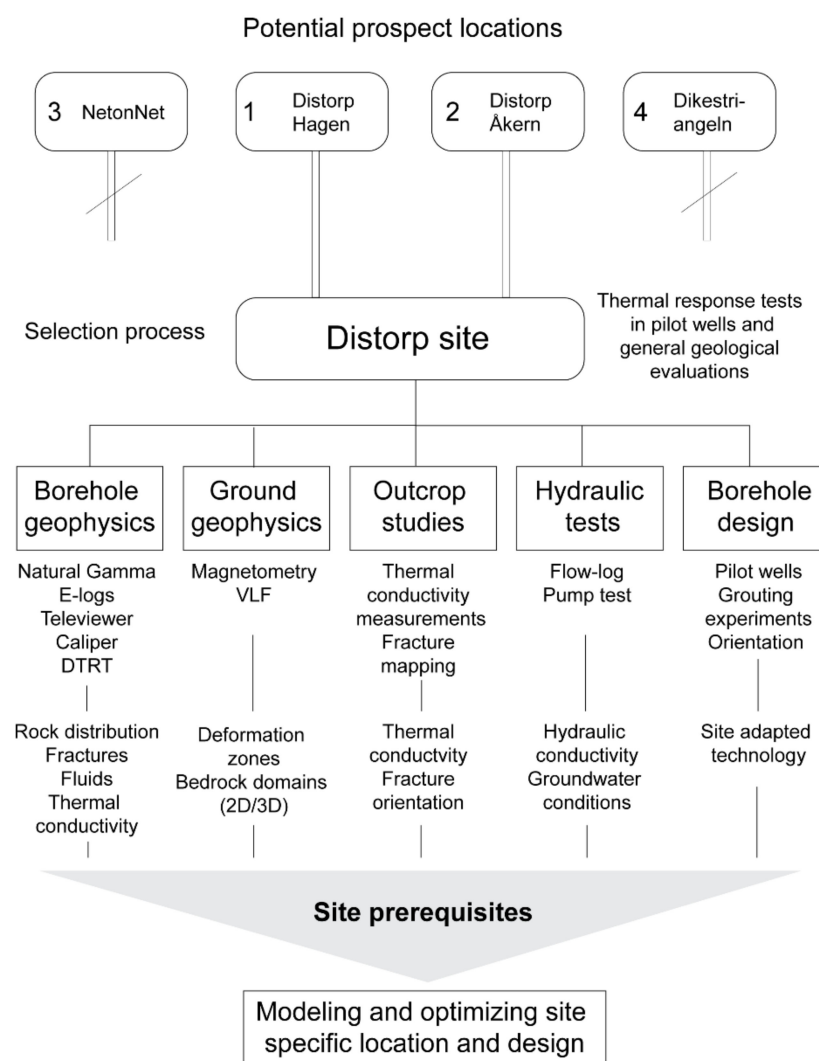


Figure 2. Diagram illustrating the various aspects of the site investigation, as well as the methodologies used. The parameters obtained from the various investigations, used as input to the modeling and site assessment are also shown. The different prospect locations are shown in Figure 1.

The main objectives for the in-depth multidisciplinary studies in the Distorp site were: (1) To apply a range of different methods to obtain the best possible characterization of the Distorp site with the resources available to the project; and (2) to evaluate these methods with regards to their suitability and capacity to provide essential information required for optimizing the modeling, site selection, and design of the final HT-BTES

system. This was done to improve the understanding of the applicability of these methods to future BTES projects.

The in-depth multidisciplinary studies started in late 2018, beginning with a detailed geological and geophysical survey of the boreholes. Initially, descriptions of the cuttings collected every three meters in the two 300 m deep boreholes Distorp Åkern and Distorp Hagen were made. Furthermore, geophysical wireline logging was also performed in the two boreholes. During 2019 and 2020, geological observations and ground geophysical measurements were performed. This included geological descriptions of the rock types at outcrop, sampling for petrophysical and measurements of the thermal conductivity on rock samples, as well as measurements of the natural gamma radiation and magnetic susceptibility. Additionally, magnetic field and VLF (Very Low-Frequency) measurements were collected across the study area. Some outcrops were photographed using a drone to generate high resolution orthographic images for fracture interpretation. Figure 3 shows a map with the location of data acquired during this work. Note that the black dashed line highlights the study area in the figure.

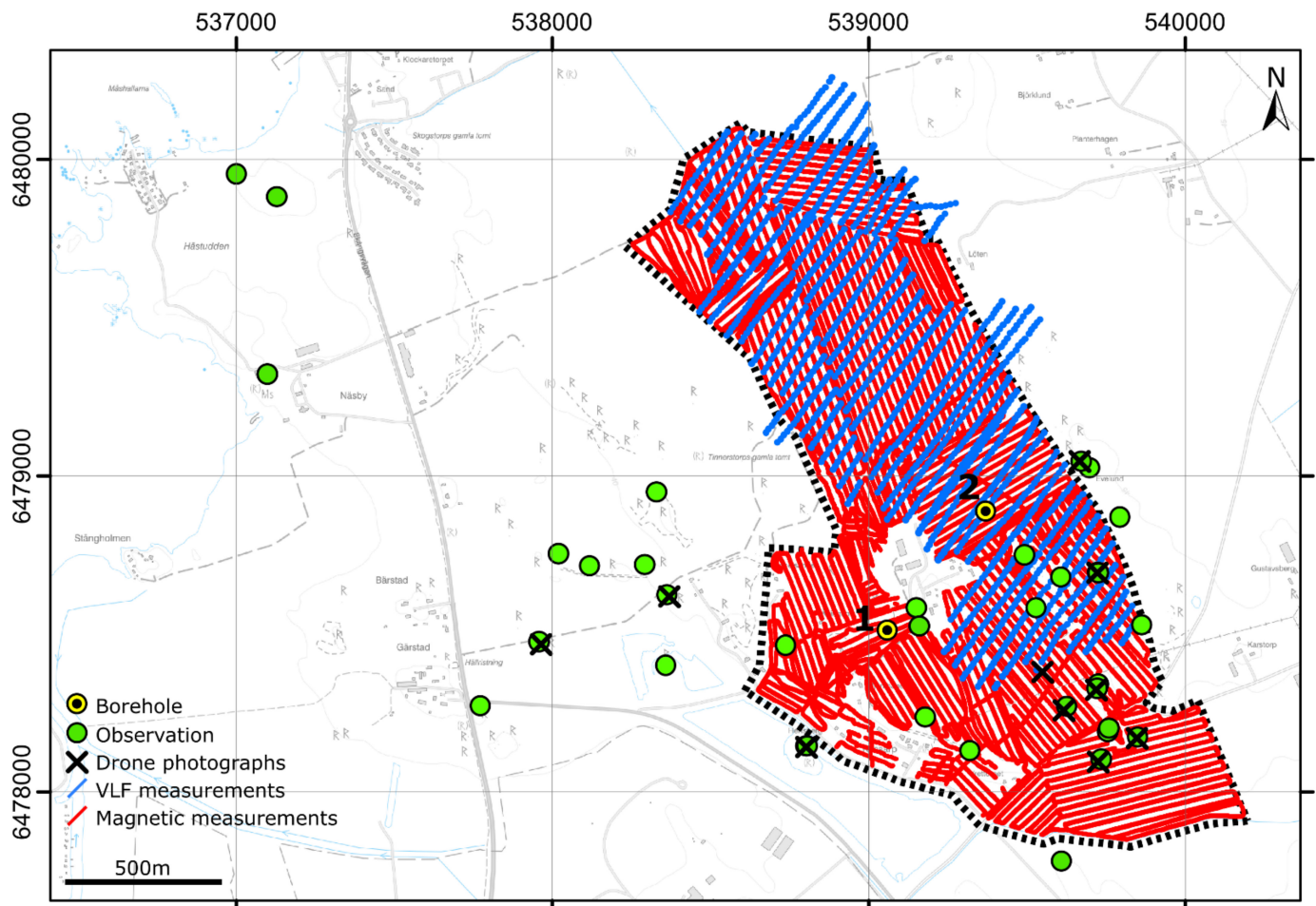


Figure 3. Base map showing the location of data acquired during this study. Borehole 1: Distorp Hagen, 2: Distorp Åkern.

Although this study addresses many methods, it is important to note that the data were collected across a range of projects with varying scopes and resources. Hence, the data collection strategy across the lifetime of the site investigation has been somewhat suboptimal. For example, the investigation wells and the TRT and DTRT were already performed prior to most of the surface measurements and analyses. As a result, the flow chart in Figure 2 illustrates a parallel execution of the methods, which was the case in this study. Ideally, this would not be the case for an optimized pre-investigation strategy,

where data from different methods would be acquired sequentially and used to inform and guide decisions throughout the workflow. Hence, ideally, the placement of the investigation wells would be decided and optimized based on the surface measurements, instead of being placed arbitrarily, as they were in this study.

A table summarizing the methods and equipment, as well as brief comments about accuracy and resolution, is provided in the supplementary data (Table S1).

3.1. Ground Geophysics

Variations in subsurface composition or rock type are often associated with changes in physical properties. Through physical measurements (for example, the magnetic or gravitational field), ground-based geophysical methods aim to characterize these variations in physical properties, and hence, infer changes in the subsurface composition. Often these measurements can be performed relatively quickly across an area. Furthermore, they do not require the bedrock to be exposed. Hence, together with bedrock observations at outcrop and borehole data, ground-based geophysical methods can be a powerful tool to map the bedrock geology over an area.

Ground-based magnetic field measurements can be made to infer variations in the magnetic properties of the subsurface. Some rock types which are highly magnetized can give rise to anomalies in the total magnetic field, which can be measured and mapped across an area. In the case of induced magnetization, the strength of the observed anomaly is related to the magnetic susceptibility of the rock [24]. The Very Low-Frequency method is an electromagnetic geophysical method that utilizes radio frequencies within the range of 3–30 kHz. If an electrically conductive subsurface structure exists, with an appropriate size and orientation to the incoming radio waves, an electrical field will be induced within the subsurface conductor. This electrical field, in turn, gives rise to a secondary magnetic field, which can, in turn, be measured. Hence, VLF measurements can be utilized to infer the presence of conductive subsurface structures, such as water-bearing fracture zones [24].

Airborne magnetic field and VLF measurements are available from the study area, collected in 1999 and 2003 by SGU as part of bedrock mapping projects. These data indicate the presence of regional deformation zones, as well as variations in the magnetic susceptibility of the bedrock within and around the Distorp area. However, these data do not provide the level of resolution required for this study, hence, ground-based magnetic field and VLF measurements were collected over the study area.

The ground-based magnetic field and VLF measurements were collected using a GEM GSMV-19 instrument. For the magnetic measurements, data points were collected continuously at one second intervals whilst walking along profiles with a nominal spacing of about 30 m (Figure 3). After acquisition, the data were corrected for diurnal variations using base station measurements from SGU's Fiby observatory. Minor line-leveling and filtering corrections were also then applied to the data.

VLF measurements were collected every 15 m along a series of profiles with a nominal spacing of 40 m. A profile azimuth of 30° and VLF frequencies of 19.6 and 24.0 kHz were used, to be sensitive to potential deformation zones with an NW–SE-orientation. A VLF frequency of 16.4 kHz was also measured to provide measurements from an approximately orthogonal direction to the first two frequencies. Power lines located in the southern part of the study area generated too much noise for data to be collected. Hence, VLF data was only acquired in the central and northern parts of the study area (Figure 3). After acquisition, some simple filtering was applied to the data before it was inverted to generate a 3D resistivity model of the subsurface. As the terrain across the study area is primarily farmland, the magnetic and VLF measurements could be collected relatively quickly and efficiently over about 5–7 days.

In addition to the VLF and magnetic field measurements, natural gamma radiation was measured at several outcrop locations using a handheld RS-125/230 spectrometer. A minimum of three measurements was made for each rock type at the outcrops, which were

investigated. Based on these measurements, the spectrometer estimates the amounts of potassium, uranium, and thorium in the different rock types.

Ground-based gravity surveying can be a powerful method for characterizing variations in bedrock geology. With this method, local anomalies in the earth's gravitational field can be used to infer changes in subsurface density [24]. Regional gravity data has previously been acquired across the Distorp area and is available from the Geological Survey of Sweden [25]. However, the average spacing between measurement points for this part of Sweden is about 2.5 km. Hence, only one gravity measurement was performed within the study focus area. Therefore, the resolution of these regional gravity data is too low for detailed mapping of the geology at the Distorp site. Acquisition of additional ground gravity measurements likely would have contributed to our assessment of the site. However, due to limitations in resources and accessibility of the measurement equipment, this was not performed as part of this study.

3.2. Drone Photography of Outcrops

A Mavic 2 pro drone was used to take photographs of several outcrops within the study area for the purpose of generating detailed orthophotos (orthographic composite photos) for fracture interpretation. During acquisition, the drone was flown at a height of 10 m, and a series of pictures was collected over the outcrop of interest using a front overlap of 80% and side overlap of 60%. The images were later processed in photogrammetry software to generate georeferenced orthographic images. The orthophotos of each outcrop were then imported into GIS software (ArcMap 10.7.1) where the fractures were mapped. Subsequently, a custom MATLAB (R2020b) script was used to perform a statistical analysis of the interpreted fractures and generate diagrams for visualization of the results.

3.3. Thermal Conductivity Measurements

The thermal conductivity of the various rock types occurring in the investigated area has been measured by the Geological Survey of Sweden using a Thermal Conductivity Scanner (TCS). The equipment used is manufactured by Lippmann and Rauen GbR in Germany. In total, 17 rock samples from outcrops inside or in the proximity of the Distorp site were analyzed. In some cases, multiple measurements were performed on a single sample, to scan in different orientations. This led to a total of 23 measurements being made for the Distorp area. The TCS measures the thermal conductivity (TC) and thermal diffusivity (TD) by applying optical scanning technology to plane or cylindrical surfaces (along the cylinder axis) of rock or core specimens. The TCS uses a focused, mobile, and continuously operated heat source in combination with infrared temperature sensors [26]. These sensors measure the sample temperature before and after heating. Typically, two reference probes with known thermal properties are analyzed together with the sample. TC and TD are determined by comparing the temperatures assessed from the certified standard samples with temperatures measured on the rock sample.

During operation, individual TC measurements are made along a scan line at a specified sampling rate across the rock sample. From these measurements, a mean average, as well as maximum and minimum TC values are calculated for the sample. Thermal diffusivity TD can also be measured together with the TC measurements.

3.4. Petrophysical Measurements on Rock Samples

During the project, measurements of both magnetic susceptibility and density were performed on 14 samples collected from outcrops in the Distorp area, in SGU's petrophysics laboratory. The density was calculated by comparing measurements of weight and volume. The weight of the samples was measured using a precision scale (FX-3200) and the volume using the Archimedes principle (displacement of water). The magnetic susceptibility was measured using a GTK K4/GSF-93 instrument, built by the Finnish Geological Survey (GTK). Here the magnetic susceptibility is measured using the deviation method, utilizing an AC bridge. Based on repeat measurements of a typical bedrock

sample, of standard size and relatively low susceptibility, the standard deviation of these instruments is about 5 kg/m^3 and $20 \times 10^{-6} \text{ SI}$ for density and magnetic susceptibility, respectively. In addition to these lab measurements, magnetic susceptibility was measured at outcrop locations using a hand susceptibility meter (SM20). To assess the variability and obtain a representative average value, at least 10 measurements were made at different points across each outcrop location.

Furthermore, pre-existing petrophysical data and outcrop magnetic susceptibility measurements from the Distorp site and surrounding area were extracted from SGU's databases. These pre-existing data were combined with the newly acquired data to form a petrophysical database for use in this study.

3.5. Wireline Logging

The wireline logging was performed by Engineering Geology at Lund University with equipment from Robertson Geologging Ltd. Two runs were performed in each borehole, the first with Natural Gamma, Temperature, Long and Short Resistivity, Single Point Resistance, and the second with Acoustic Televierer (ATV).

The Natural Gamma log is the most widely used log for lithological characterization of successions within boreholes. The log is a passive radiometric log that uses a scintillation counter that detects the natural gamma radiation coming from the rocks in the borehole wall [27]. The radiation originates from the potassium-40, radium-uranium, and thorium series. For crystalline rocks like granites and metabasites there is a significant difference in the potassium content, which can be detected in the Natural Gamma log. The relatively potassium-rich granites (high in mica and feldspars) will consequently result in a higher gamma-ray level in comparison to the generally potassium-poor mafic rocks [28]. The purpose of this log was, with the support from descriptions of the rock cuttings, to get a detailed picture of the rock type distribution in the boreholes. The gamma-ray results can also indirectly be used as a measure of the thermal properties of the rocks within the borehole, since most in situ heat production are related to the amount of naturally occurring radioactive elements mentioned above [29].

The Single Point Resistance tool measures the electrical resistance of the subsurface in the immediate vicinity of the borehole. The tool operates by measuring the difference in voltage between two electrodes using a constant current. Single-point logs are sensitive to the resistivity of the lithology adjacent to the electrodes, regardless of electrical influences caused by varying thicknesses and composition of beds; thus, they have, in general, a very high vertical resolution.

The Short and Long Resistivity tool measures (as opposed to resistance) the resistivity of the formation volume (rock and formation fluids) outside the immediate proximity of the borehole. The vertical resolution is less than for the Single Point Resistance tool. The tool works best in sedimentary bedrock with relatively thick beds where the focus lies on determining the thickness of the mud invaded zone in porous rocks, as well as properties of any reservoir fluids present.

Several properties affect the resistivity of a rock volume, for example, porosity, the resistivity of the fluid within fractures and pores, mineral composition, and the texture of the rock. Granitic rocks have, in general, slightly lower resistivity compared to mafic rocks. Although, it should be noted that there is a significant variation in the resistivities of mafic and felsic intrusive rock types [30].

The Acoustic Televierer generates an acoustic image of the borehole wall by detecting the arrival time for a reflected sound wave generated by a rotating piezoelectric source. Besides the arrival time, the log registers the amplitude of the measured acoustic wave. The measurement gives a continuous, 360 degrees image of the borehole wall, which is geographically orientated. After processing, fractures and variations in the density of the borehole wall can clearly be identified. A major advantage of the Acoustic Televierer is that it can be run in boreholes where the drilling fluid is opaque, for example drilling mud. Within this project, Acoustic Televierer data has been used to map the in-situ fractures

to assess the hydraulic properties, borehole integrity and to determine the deviation and direction of the investigation boreholes. Vertical boreholes with minimal deviation are essential in a multiwell HT-BTES where the distance between the individual boreholes is commonly only a few meters. Too much deviation can cause undesirable thermal interaction between boreholes, as well as increase the risk of collision between boreholes during drilling operations [31].

3.6. Thermal Response Tests

Thermal measurements, including thermal response tests and distributed thermal response tests, were performed. Conventional TRT is a relatively simple and well-established pre-investigation method in the shallow geothermal industry. It is utilized for quantifying effective underground properties, and thereafter, provides input for system design [32].

TRTs are commonly performed by injecting the heat into the borehole at a constant rate by circulating a heated secondary fluid through a closed-loop borehole heat exchanger. The effective thermal conductivity (λ^*) and effective borehole thermal resistance (Rb^*) are estimated through an inverse modeling procedure. During this process, measurements of the heat exchanger inlet- and outlet temperature in response to the heat injection over time are matched with the equivalent temperature response obtained from a parameterized model. For this purpose, under the common assumption of pure conduction heat transfer in a homogeneous medium, the infinite line source (ILS) model was used [33]. This test procedure implies that the experimental data and the best-fit parameter values obtained only represent spatially averaged predictions of the thermal characteristics of the subsurface and BHE performance. In other words, no information about subsurface heterogeneity is provided.

Application of distributed temperature sensing (DTS) technology, based on Raman optical time-domain reflectometry allows for downhole temperature measurements to be recorded along the full length of the borehole during the response test. One or multiple fiber optic cables may be installed in the test borehole, while performing a TRT. The processed temperature data acquired from the DTS system consist of discrete (averaged) representations of the continuous temperature distribution over a sampling interval. The sampling resolution, i.e., the sampling interval spacing over which signals are collected and averaged along the fiber, can be as low as 0.125 m for high performance devices [34]. Distributed temperature measurements can also be carried out with other types of sensors, but optical fiber cables, when properly used, offer significant advantages [35]. This type of TRT is often referred to as a Distributed Thermal Response Test.

In contrast to conventional TRT, based on BHE inlet- and outlet temperature measurements, the DTRT permits evaluation of λ^* and Rb^* locally along the borehole using time series of downhole temperature profiles acquired from DTS data as input to the response model [36]. The DTS instrument used in this study has a sampling resolution of 203 cm, which enabled TRT evaluation at around 150 sample intervals along the two 300 m deep investigation wells. Temperature profiles are also obtained during the test phases before and after heat injection, which allow for evaluating additional factors that affect the temperature conditions in the borehole, such as vertical groundwater movement and the presence of water-bearing fractures. Passive DTS measurements taken under undisturbed ground conditions can be used for characterizing near-surface seasonal temperature propagation effects, and at greater depths, the geothermal gradient.

3.7. Hydraulic Tests

Hydraulic tests were performed in connection with an experimental grouting project conducted in parallel with the present study [23]. The aim of the field experiments was to explore the use of permeation grouting techniques to implement open-loop BHEs. The primary objective of the hydraulic tests was to characterize near-borehole hydraulic conditions in the rock mass.

In the 240 m and 300 m deep Distorp Hagen wells, the hydraulic testing procedure involved the performance of single-hole, short-duration water loss measurements, which were carried out by injecting water into the test section under a constant pressure of 200 kPa. The pressure was maintained until the injection flow rate had stabilized (i.e., reached quasi-stationary condition), which typically occurred within time periods of the order of minutes. The pressure and flow data were evaluated through steady state flow analysis using Moye's formula to estimate a transmissivity value for the test section [37].

A double-packer system was used to isolate sections of interest within the borehole to perform the investigation. Measurements using 50 m section lengths were performed at regular intervals between about 10 m depth and the base of the borehole. Additional measurements were also carried out using a smaller packer spacing of 5 m in four sections within the shallowest 50 m of the borehole. These sections were selected based on the wireline logs, which indicate intervals with a high fracture density or the occurrence of single conductive water-bearing fractures.

4. Results

4.1. Bedrock Composition and Thermal Properties

The dominant rock types expected within the site area are, according to the bedrock map [18], grey and red fine- and medium-grained granite, greyish granite-granodiorite, and dark grey to black gabbro and metabasite (Figure 1). Different orogenic phases with granitoid intrusions deformation and metamorphism have resulted in a heterogeneous rock mass which in places also consist of folded migmatite gneiss.

The regional bedrock map (Figure 1) shows that smaller areas with metabasite and gabbro occur in the southeastern most parts of the site area, while most of the bedrock surrounding the investigation wells is composed of fine-grained red and grey granite. In the northwest parts of the site, the bedrock is dominated by variably gneissic granite and granodiorite. However, it should be noted that there are relatively few outcrops in the northern part of the area where geological observations can be made. Hence, the map in this area is primarily based on regional geophysical data and is consequently somewhat uncertain [18]. Most outcrops occur in the southeast and southern part of the study area. In total, 22 of these outcrops, dominated by variably grey and red, fine- and medium-grained granite, were sampled in this study (Figure 3). In addition, a few outcrops with mafic rocks were sampled to the southeast and west of the site area.

Considering the regional bedrock map, the composition of the uppermost bedrock within the site area should be dominated by various granitoid rock types with minor volumes of mafic rocks. Hence, an average thermal conductivity close to that of granite would be anticipated across the study area. Thermal data within a c. 5 km radius from the Distorp site, based on modal mineralogical analysis of rock samples, indicate that the average thermal conductivity for the granites in the area is 3.36 W/mK (Std Dev 0.20 W/mK), while the mafic rocks show an average of 2.61 W/mK (Std Dev 0.14 W/mK). Results from the laboratory TCS measurements on rock samples from the study area fall within the same range as the values from the modal-based regional database. A statistically reliable relationship between thermal conductivities based on modal mineralogical analyses and results from TCS-measurements have also been shown by [38]. The TCS-analyses give a mean thermal conductivity of 3.08 W/mK for the granites, while the mafic rocks give a significantly lower mean value of 2.42 W/mK (Figure 4). The results from the thermal conductivity lab measurements and the calculated values from modal analyses are presented as supplementary data (Tables S2 and S3).

a) Granitoids

b) Mafic rocks

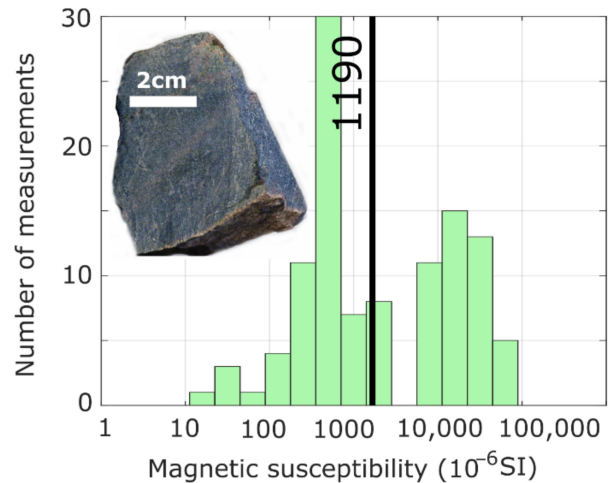
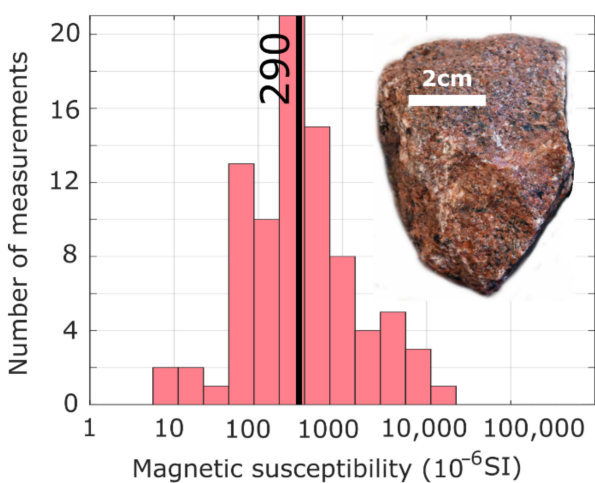
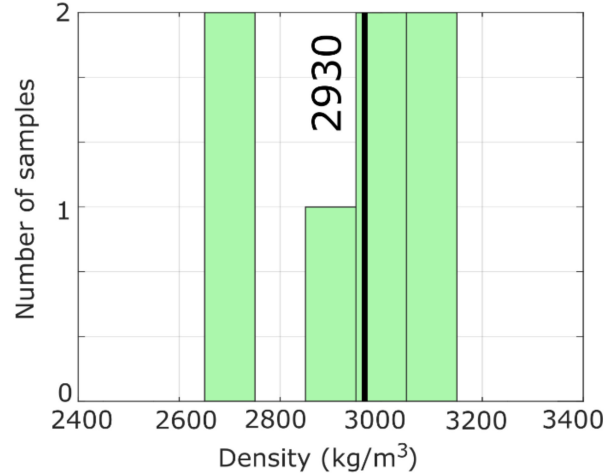
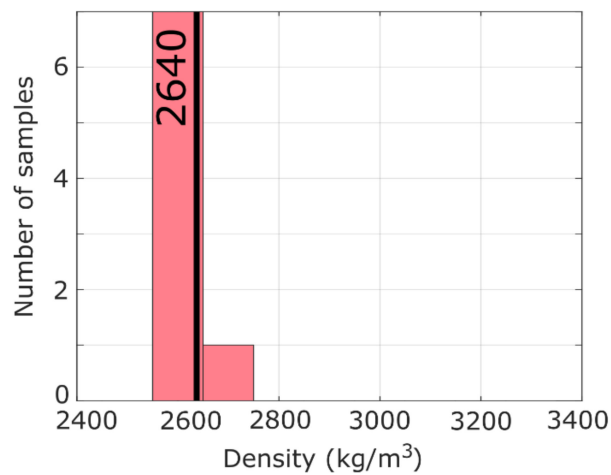
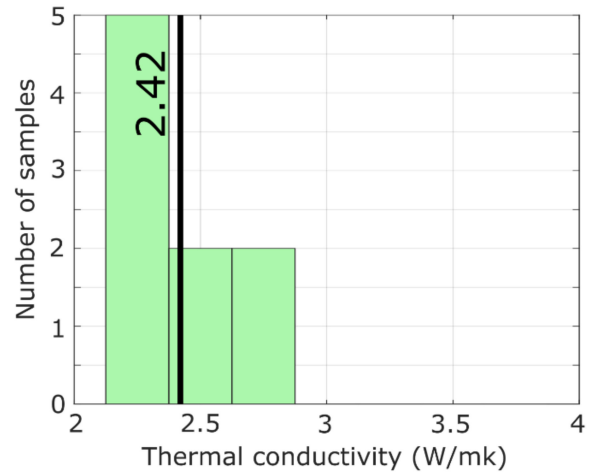
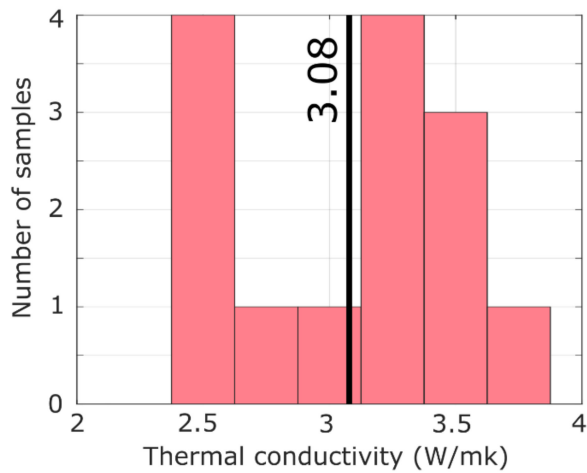


Figure 4. Petrophysical data for granite and mafic rock types. Histograms showing thermal conductivity data (**top**), density data (**center**), and magnetic susceptibility data (**bottom**), are shown for each rock type. The thick black lines display the average values for each plot. The mean average value is shown for the thermal conductivity and density data, while the median average is shown for the magnetic susceptibility data. A close-up image of each rock type is shown on the magnetic susceptibility graph. (a) Graphs on the left are for Granitoids. (b) Graphs on the right are for Mafic rocks.

The two 300 m deep investigation wells reveal that the subsurface bedrock mass is not as uniform as expected from the bedrock map. It should be noted especially that the two wells show quite different rock successions, despite being in the same type of granite on the geological map. The DTRT measurements also demonstrated differences in thermal conductivities that relate to the rock type distribution in the two wells. The Distorp Åkern well gave thermal conductivities between 3.09 and 3.58 W/mK with an average of 3.30 W/mK (Figure 5), while the Distorp Hagen well had values ranging between 2.85 and 3.64 W/mK with an average of 3.43 W/mK (Figure 6). TRT measurements show that the effective thermal conductivity at Distorp Hagen is slightly lower than Distorp Åkern, with values of 3.05 and 3.28 W/mK, respectively. The error in this type of in situ thermal conductivity measurement is known to be 5–15% [39]. Although it is possible that error in the presented results is within this range, it should be noted that the thermal conductivity values above have been measured/calculated during the heat injection phase of the DTRT and that the injected heat per unit length has been assumed to be the same in all sections of the borehole. In [36], it is stated that firstly, higher accuracy is obtained when tests are evaluated during thermal recovery after heat injection (with no radial temperature gradient in the borehole and avoiding the presence of thermosyphon effects). Secondly, it is stated that local thermal conductivity calculations should be performed using local heat injection rates, which were not measurable in the tests presented in this paper. The increase of thermal conductivity with depth observed in one of the two boreholes and the difference between average thermal conductivity values from the DTRT and the effective value obtained from a standard TRT are attributed to these two factors. More details about the factors affecting TRT results can be found in [39,40]. DTS data obtained during TRT on the Distorp Åkern well are provided as supplementary material (Spreadsheet S1).

When comparing the natural gamma logs for the two wells, a clear difference can be seen in the measurements. The gamma response is mainly related to the presence of potassium in these types of rock. Hand spectrometer measurements give a mean potassium content of about 4.0% for the granites, while the mafic rocks have a potassium content of about 2% (Supplementary Table S4). Relatively low gamma values are thus interpreted to represent rock types with a lower amount of potassium, thus primarily mafic rock types in this geological setting. Hence, the regions with low gamma values, within the somewhat variable gamma signature are interpreted to indicate metamafic or gabbro rocks in the Distorp Åkern well. It was also indicated in the cuttings material that there is a greater volume of mafic rocks occurring in the Distorp Åkern well (Figure 5) than in the Distorp Hagen well (Figure 6). In the Distorp Hagen well, the gamma values are on average higher than in the Distorp Åkern well and exhibit less variability. This is interpreted as a more homogeneous sequence of granite and granodiorite. This interpretation is also verified by the cuttings that indicate a relatively homogeneous rock succession of fine- and medium-grained granite in this well.

The difference in the number of mafic rock types encountered in the two wells and the associated thermal rock properties lead to a different thermal response in the two wells.

Based on the petrophysical data from this study, a significant difference between the magnetic properties of the granitic and mafic rocks exists (Figure 4). Here it can be observed that in the histograms, both rock types have a peak at about 300×10^{-6} SI, which is most likely due to the presence of iron-bearing paramagnetic minerals (such as biotite). However, the mafic rocks have an additional peak at about $20,000 \times 10^{-6}$ SI, which is likely due to the presence of magnetic minerals (such as magnetite). Hence, strong magnetic anomalies within the study area are likely to be associated with mafic rock types. Figure 7 shows maps of the total magnetic field over the study area, and the average resistivity of the upper 300 m of the subsurface. The black dashed line highlights the study area in the figure.

Distorp Åkern

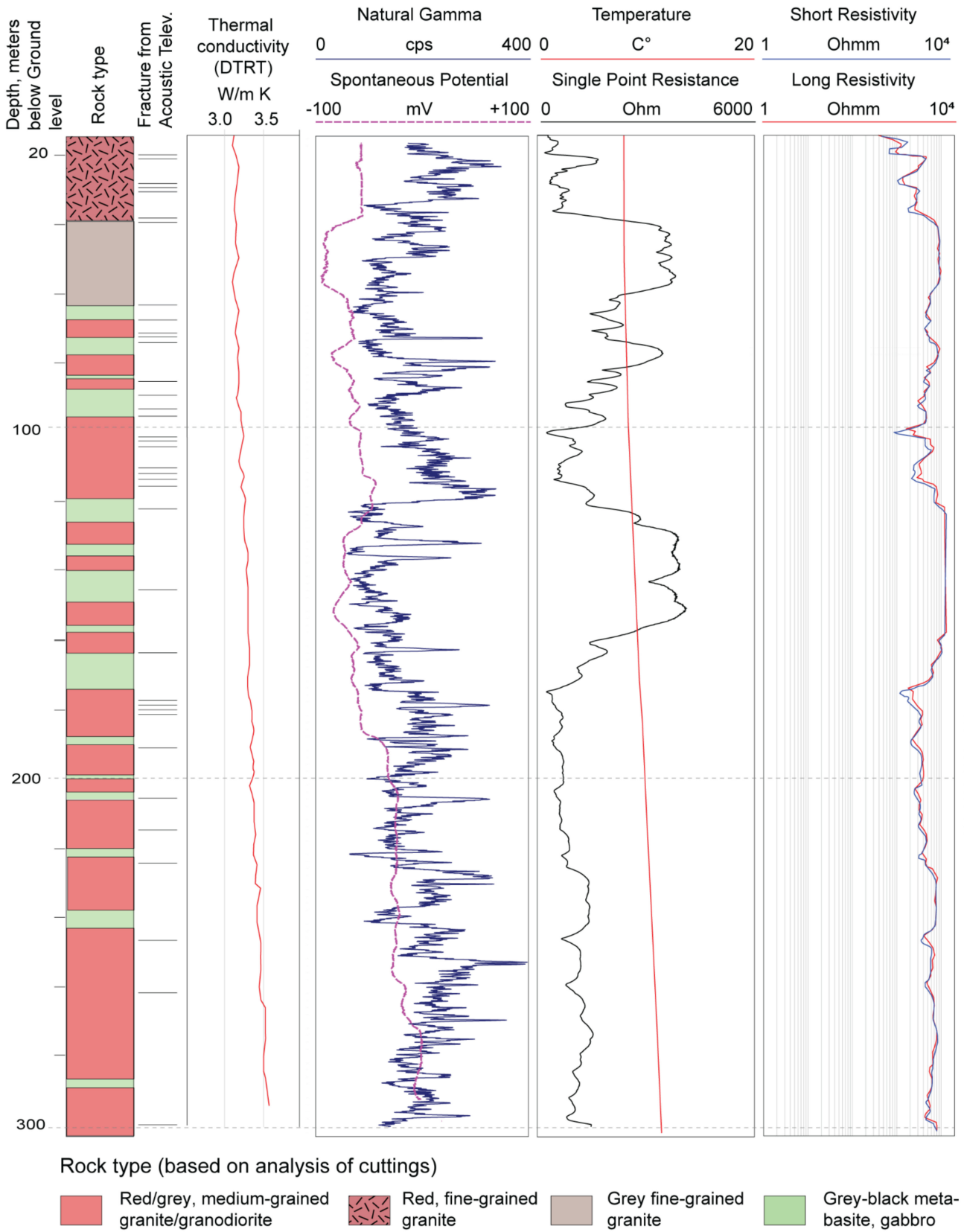
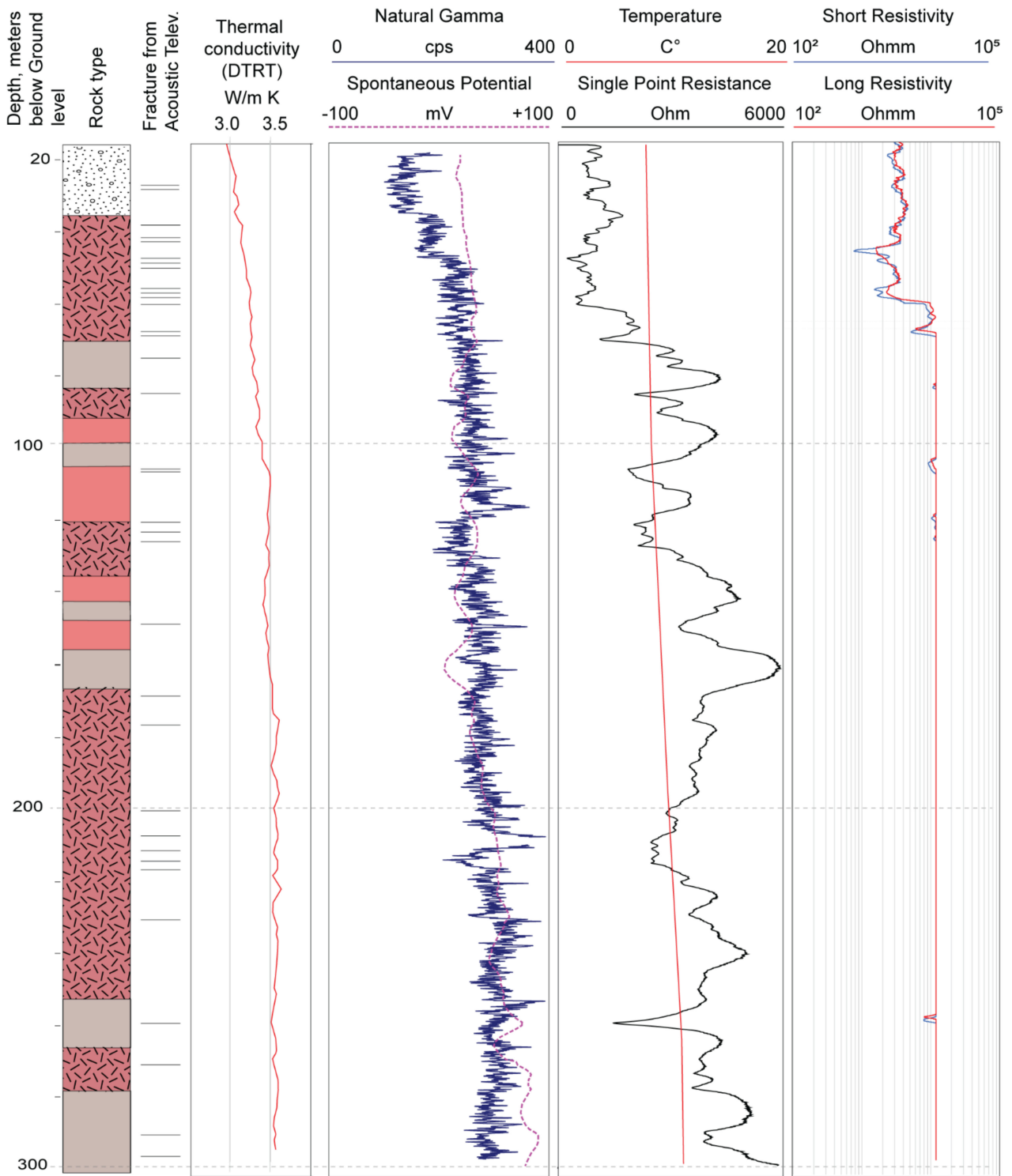


Figure 5. Composite log of the 300 m deep Distorp Åkern well.

Distorp Hagen



Rock type (based on analysis of cuttings)

- Red/grey, medium-grained granite/granodiorite
- Red, fine-grained granite
- Grey fine-grained granite
- Sandstone

Figure 6. Composite log of the 300 m deep Distorp Hagen well.

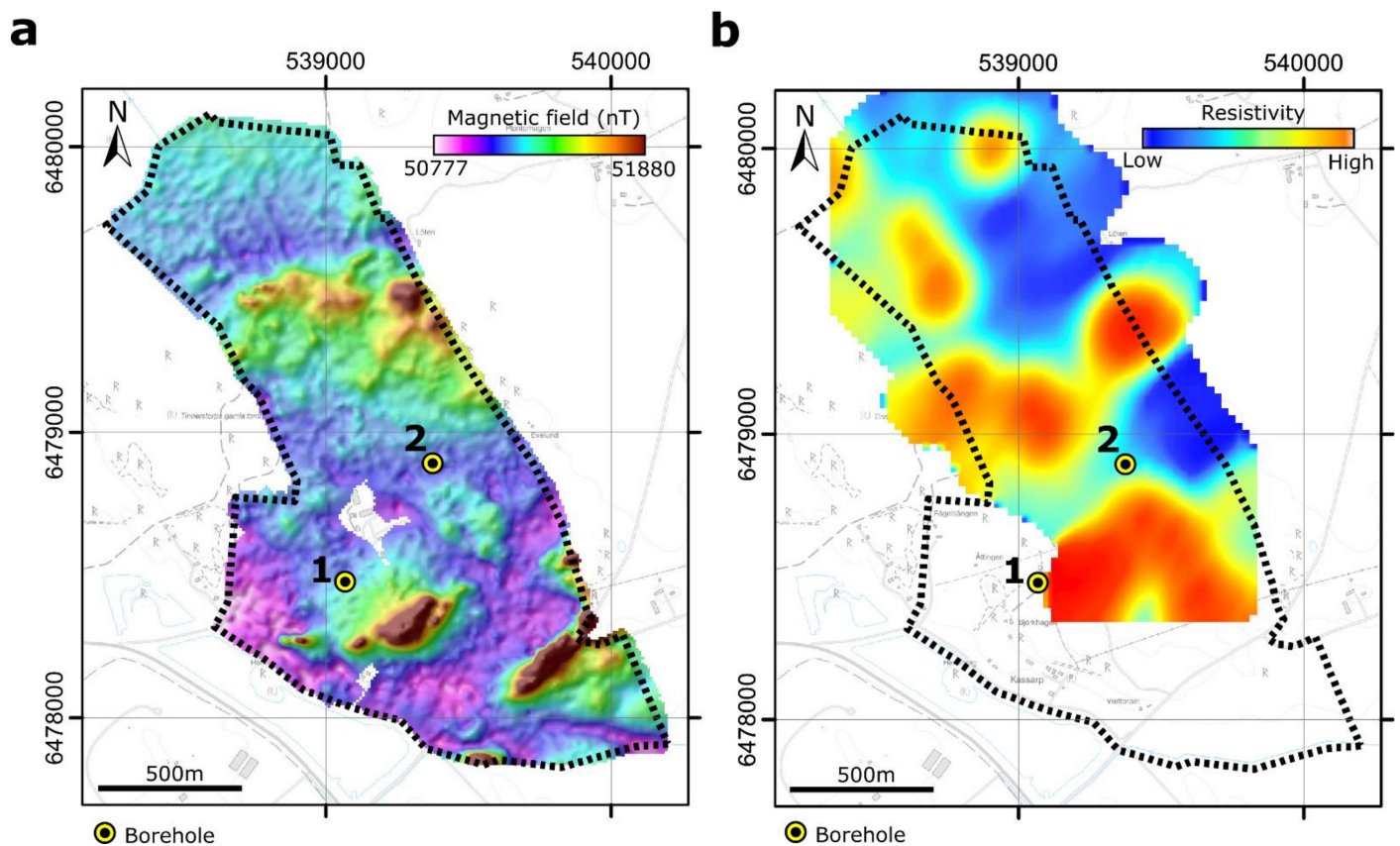


Figure 7. (a) A map of the total magnetic field over the study area. (b) Map of the average resistivity of the upper 300 m of the subsurface derived from the 3D resistivity model generated from VLF measurements. Borehole 1: Distorp Hagen, 2: Distorp Åkern.

On inspection of the map of the magnetic field measurements (Figure 7a), several regions with positive magnetic anomalies (relatively high values) can be identified in the southern part of the study area. These anomalies coincide with outcrops where mafic rocks have been observed. Hence, considering the petrophysical data, it is likely that these positive magnetic anomalies are due to the presence of mafic rocks. A broad positive magnetic anomaly is also present to the north of the Distorp Åkern well, which can also be interpreted as a region with more mafic rock types. Such an interpretation of this anomaly is supported by outcrop observations to the west of this anomaly, where isolated units of mafic rocks have been mapped within the predominantly granitic rocks. The remaining parts of the study area characterized by relatively low magnetic field values can be interpreted to be predominantly granitic rocks. Figure 8 shows a detailed interpretation of the bedrock geology of the study area based on the new data collected in this study, here the regions of more mafic rock types (green) are interpreted to correspond broadly to regions with high magnetic field values.

In the magnetic field data shown in Figure 7a, several linear zones can be identified, over which a sharp change in the magnetic field values occurs (discontinuities). These are most notable in the southern part of the study area. Specifically, two zones with an NW–SE-orientation exist; the first is located between the two investigation wells, while the second lies about 300 m south of the Distorp Hagen well. A more subtle discontinuity in the magnetic data with an N–NW-orientation can be interpreted about 100 m to the west of the Distorp Hagen well. These are interpreted to represent deformation zones over which the geology has been displaced and are shown in Figure 8 as black lines. The orientation of these discontinuities is consistent with the large-scale deformation zones mapped from airborne geophysical data (Figure 1).

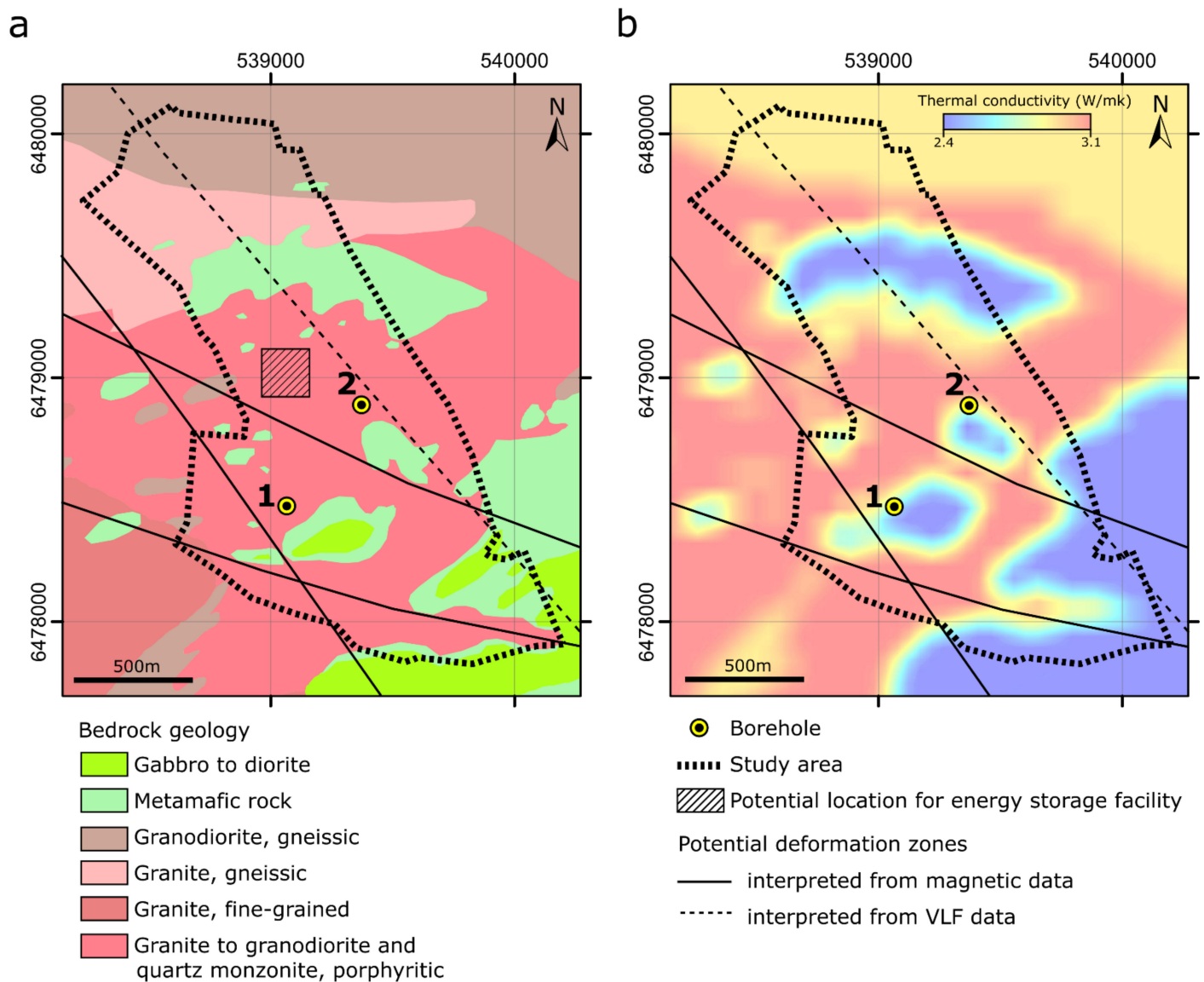


Figure 8. (a) Interpretation of the Bedrock geology based on geological and geophysical observations made in this study. A potential location for the energy storage facility is highlighted. (b) A map showing the prognosed bedrock thermal conductivity based on the data and observations from this study. Borehole 1: Distorp Hagen, 2: Distorp Åkern.

On inspection of the resistivity map, generated from the VLF data shown in Figure 7b, a general transition from higher resistivities in the west to lower resistivities in the east can be observed. This is interpreted to be largely due to variations in the surface sediment layer, where more resistive sandy and silty moraine are mapped to the west, and less resistive glacial clay is mapped to the east of the study area. Furthermore, several high resistive anomalies can be observed in Figure 7b. Two of these, one to the southeast of the Distorp Åkern well and another to the northwest, correspond to areas where outcrops exist. Hence, these can be interpreted as regions where the resistive bedrock is relatively close to the surface, and the more conductive sediment layer is thin. A linear region with relatively low resistivity values and an NW–SE-orientation can potentially be interpreted in the resistivity map. This zone is most notable directly to the north of the Distorp Åkern well, where it intersects a region of relatively high resistivity. This zone could potentially indicate the presence of a more conductive zone in the bedrock, such as a water-filled fracture system (deformation zone). This potential zone is shown in Figure 8 as a dashed black line.

If both the detailed bedrock interpretation of the study area (Figure 8a) and the thermal conductivity lab results (Figure 4) are considered, it is possible to make a simple prognosis

of the thermal conductivity of the bedrock across the study area, which is shown in Figure 8b. Here the mean average thermal conductivities (from the TCS measurements) of 3.08 and 2.42 W/mK are assigned to granitic and mafic rocks, respectively. An intermediate thermal conductivity was assigned to granodiorite rocks. Some smoothing was applied to account for the mixing and interlayering of these two rock types in transitional areas. It should be noted that there is significant uncertainty in this map of prognosed thermal conductivity. This is due to the large variation in thermal conductivity values measured from samples, as well as the uncertainty in the detailed bedrock map, which is based largely on geophysical data, rather than outcrop observation. Despite this, it can be a useful tool to visualize the anticipated bulk thermal conductivity values based on the updated geological map.

4.2. Fracturing and Fracture Orientation

Figure 9 shows an example of an orthophoto that was generated for an outcrop located on the southwestern edge of the study area. At this outcrop, a clear contact between coarse-grained granite and more mafic fine-grained granodiorite can be observed. An example of the fractures interpreted for this outcrop are shown in Figure 9b. Similar fracture interpretation was performed on all outcrops where drone photographs were available to generate a database of about 1500 fractures. A rose diagram showing the distribution of fracture directions, weighted by fracture length, for all fractures which were interpreted in the study is shown in Figure 9c.

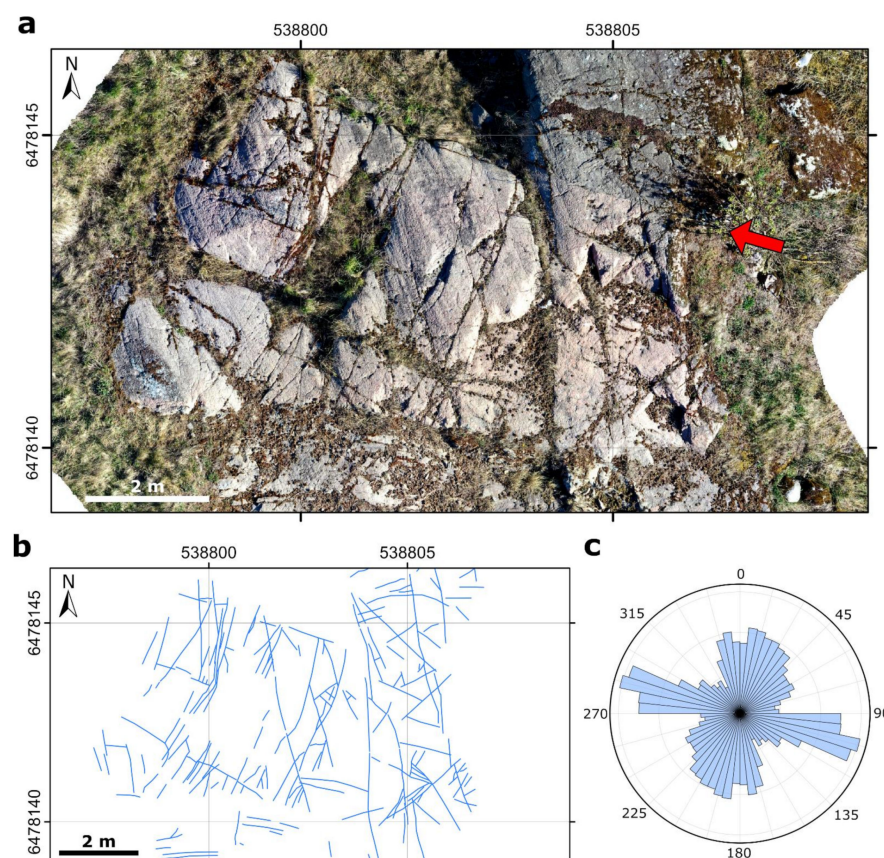


Figure 9. (a) Example section of a drone orthophoto of an outcrop within the study area. A contact between fine-grained granodiorite rocks (grey) and coarse-grained granite rocks (pink) is marked with a red arrow. (b) interpreted fractures (blue lines) for the portion of the orthophoto shown in (a). (c) Rose diagram showing the orientation of fractures mapped on all outcrops within the study area, where drone photographs were taken.

Here it can be observed the predominant fracture set in the study area has an azimuth of about 105° . Secondary fracture sets appear to exist with azimuths of 15° and 165° . A primary fracture orientation of 105° corresponds well to the orientation of the regional deformation zones mapped from airborne geophysical data (Figure 1), as well as several of the potential deformation zones mapped from the ground-based magnetic data (Figure 8). The secondary fracture set with an azimuth of about 165° corresponds well to the potential deformation zone mapped with the VLF data and one of the deformation zones mapped with the magnetic data (Figure 8).

Downhole fracture mapping by visual inspection of Acoustic Televiewer images and geoelectric data sets collected in the 300 m and 240 m deep Distorp Hagen wells indicates relatively high fracture density at shallow depths to around 60 m. Estimates of the lineal fracture density (P_{10}) [41] at discrete 1 m intervals within the depth section of 10–60 m of the boreholes are shown in Figure 10. A maximum fracture density of 7 fractures per meter can be observed in both boreholes. At larger depths, only single or groups of few fractures were identified in scattered intervals along the boreholes. Although not described in this study, additional information on fracture characteristics (e.g., strike and dip) can be acquired from Acoustic Televiewer data with additional analysis. This is possible because the tilt and orientation of the instrument are logged during measurement. The ATV image logs for both Distorp Hagen wells are provided in the supplementary data (Figures S1 and S2).

4.3. Groundwater Conditions

The estimated capacities of the two 300 m deep investigation wells within the Distorp site were 1200 L/h and 1500 L/h based on air-lift yields measured during the completion of the wells. The groundwater table is relatively shallow and was observed to be about 2 to 3 m below ground level within the study area. Borehole transmissivity data, based on hydraulic testing in the 300 m and 240 m deep Distorp Hagen wells, are presented in Figure 10. The range of estimated transmissivities, using measurement intervals of 50 m, spans from $8.4 \times 10^{-7} \text{ m}^2/\text{s}$ to $2.6 \times 10^{-5} \text{ m}^2/\text{s}$ in the 300 m deep well, and from $3.3 \times 10^{-7} \text{ m}^2/\text{s}$ to $1.0 \times 10^{-5} \text{ m}^2/\text{s}$ in the 240 m deep well. The medians of these ranges are $1.4 \times 10^{-5} \text{ m}^2/\text{s}$ and $5.3 \times 10^{-6} \text{ m}^2/\text{s}$, respectively.

A trend of decreasing transmissivity with depth can be observed. An exception to this is seen in the lowermost two sections (which overlap to some degree) of the 300 m well. Qualitative interpretation of ATV and geoelectric data indicates that the water loss within these sections is dominated by a single fracture located at a depth of approximately 260 m (Figure 10). The maximum transmissivity estimates occur in the shallowest test interval of both wells, corresponding to the regions where the maximum fracture densities are also estimated (Section 4.2). This agrees with the common observation that bedrock transmissivity is often depth-dependent. Possible explanations for this include, near-surface fracturing, due to stress release and dissolution of fracture filling minerals. Another explanation is the closure of fractures, due to increasing overburden stress at greater depth [42,43].

Thermal anomalies that can be observed in the temperature-depth profiles obtained during DTRT may be indicative of possible groundwater movements. The DTS data can provide a useful means to distinguish the flow state of fractures that are detected from geophysical logs. In the example shown in Figure 11, the combined Acoustic Televiewer and single point resistance logs indicate the presence of multiple water-bearing fractures within the considered interval (e.g., at depths of 79 m, 85 m, and 109 m, as indicated in Figure 11). However, a prominent temperature anomaly is only associated with one of these fractures, at a depth of around 85 m. Hence, the DTS temperature profile detects fractures with the most significant fluid flow. The DTS temperature profile records can also be used for quantitative assessment of cross-hole and in-hole groundwater flow velocities [44,45]. However, groundwater flow velocities based on DTS data were not addressed in this study.

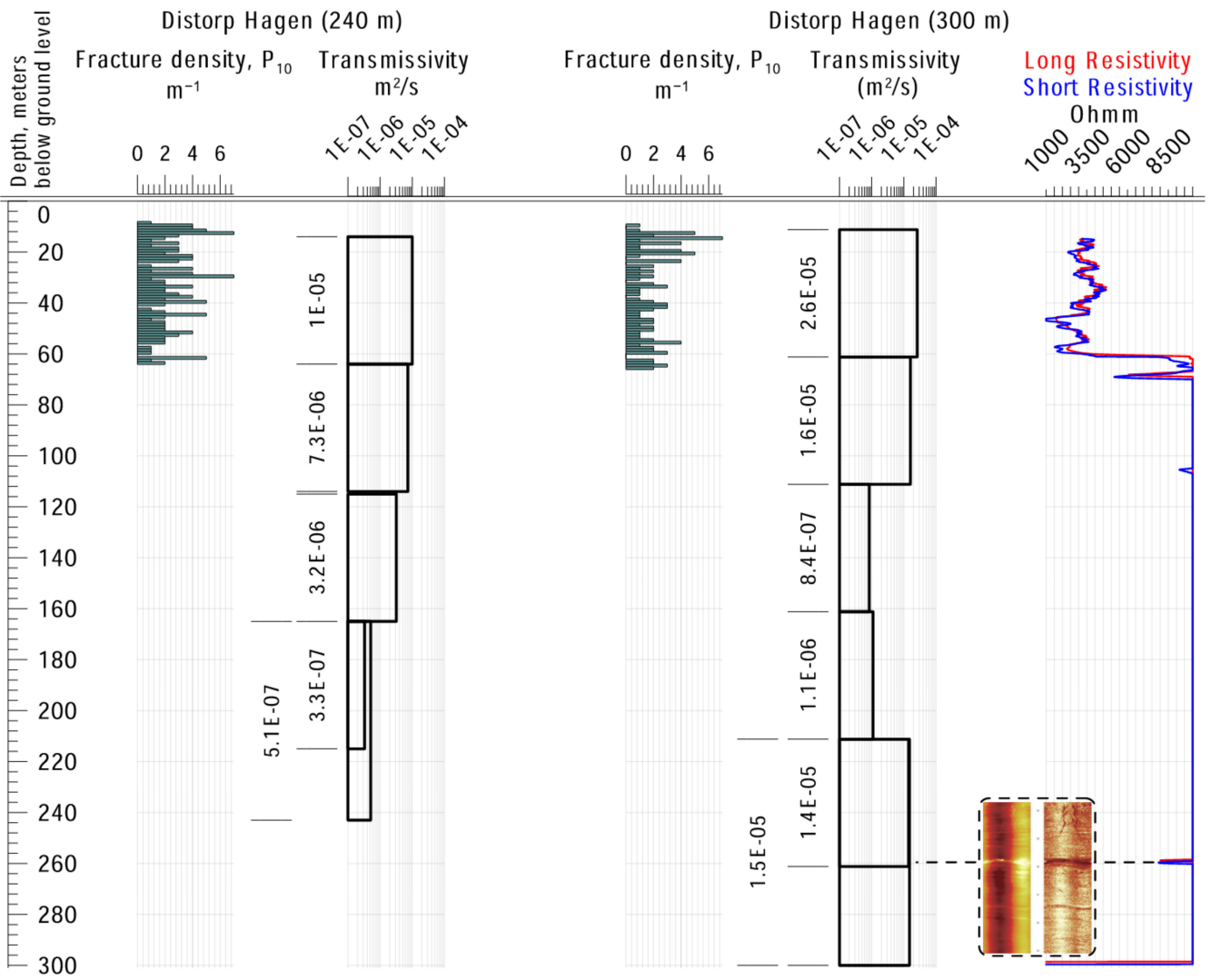


Figure 10. Transmissivity estimates with measured depth below ground level for the 240 m and 300 m deep Distorp Hagen wells.

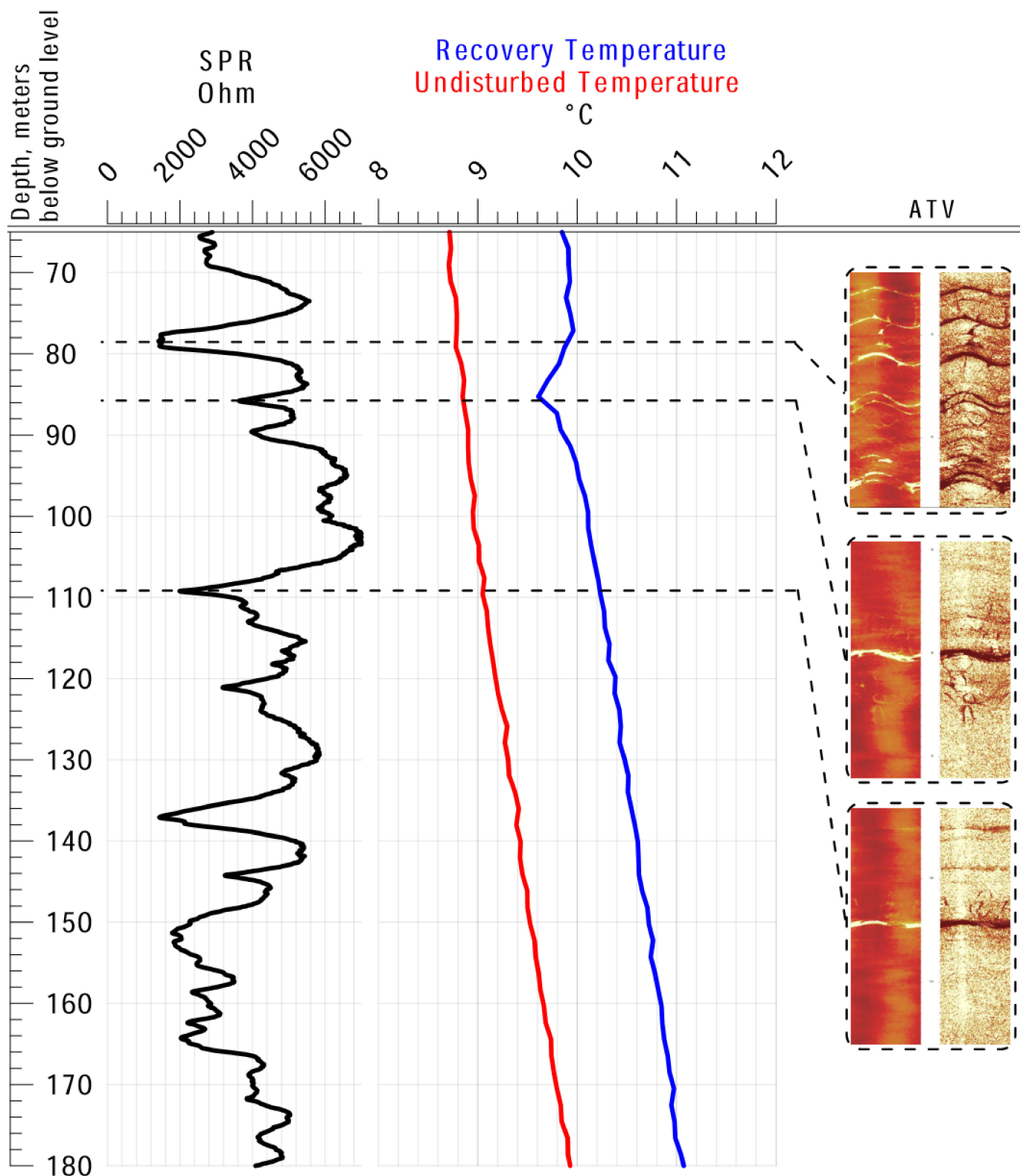


Figure 11. Detection of flowing fractures using single point resistance (SPR) logs and temperature profiles acquired during DTRT in the 240 m deep Distorp Hagen well.

5. Discussion

It is known that the investment cost associated with multiwell HT-BTES systems is substantial. As such systems may be designed and built for large scale installations,

an arbitrary assessment of design and placement, based on limited data, can lead to high risks regarding performance, longevity, and impact on the surrounding environment. Anisotropic geological conditions are especially common in a crystalline rock mass, like the conditions in the Distorp site. When considering sites with sedimentary strata, a certain degree of predictability in the geological conditions parallel to bedding is reasonable to assume, despite variability perpendicular to the bedding direction. However, the anisotropy observed in crystalline rocks is, in comparison to sedimentary rocks, often considerably greater. As a result, the anisotropy in thermal properties anticipated within crystalline rocks is also typically higher than in sedimentary rocks. The frequency and predominant orientation of fractures and fracture zones are also important factors that can have an impact on the groundwater flow, and hence, the size and shape of the rock mass thermally affected during the operation of an HT-BTES system. Hence, a strategy relying only on single investigation wells for appraisal and design of a large-scale HT-BTES facility in an anisotropic crystalline bedrock setting is unlikely to provide accurate information required to assess potential performance, longevity, and environmental impact.

To fully characterize the anisotropic geological conditions (i.e., to obtain a more solid base for design), a multidisciplinary approach in the pre-investigation phase is recommended, especially for HT-BTES systems that utilize large well clusters.

However, characterization of anisotropic conditions in a crystalline rock mass on a local scale is challenging and can be resource-demanding. Thickness and composition of the soil cover, petrophysical properties of the rock mass, groundwater conditions, and the accessibility of outcrops all govern the possibility to collect information, as well as the methods that can be applied. The approach in this study has been to test and evaluate a comprehensive range of methods that may be appropriate for improving the empirical data set on various properties in a crystalline bedrock domain. It is not recommended that all the methods addressed in this study should be applied in all pre-site evaluations. In fact, it is important to emphasize that several aspects of the data collection and investigation strategy within this study are suboptimal. This is largely because the data in this study have been collected across various separate and sequential projects, which have had varying individual scopes and objectives. For example, in this study, the boreholes were drilled prior to the surface geophysical and geological investigations. Ideally, the results of the relatively quick and resource effective ground geophysical and geological investigations should have been available to optimize the location of the relatively expensive boreholes. Furthermore, in this study, many methods have been tested in parallel to investigate various aspects of the HT-BTES site. It is recommended, however, that in future investigations, a more sequential and integrated data acquisition and analysis strategy be adopted. Hence, it is not suggested that the workflow presented in this study be considered best practice for a pre-investigation study for an HT-BTES system. Instead, we aim to showcase and exemplify a range of available methods which, if appropriate, can be selected to form part of an HT-BTES investigation strategy.

It is important to highlight that the choice of methods should be tailored to the scenario being assessed. When designing an investigation strategy, it is important to consider the physical characteristics of the bedrock, as well as the anticipated level of subsurface uncertainty when selecting methods. The limitations of the different methods should also be considered. Furthermore, the investigations should be of an appropriate scale, bearing in mind the resources available for the project and the eventual size of the HT-BTES system. Finally, the investigations should form part of an integrated and sequential site evaluation strategy.

In the following discussion, the performance and limitations of the different methods applied at the Distorp site are discussed, with the aim of providing information that can be useful for the design of pre-site investigations strategies for future HT-BTES systems within crystalline bedrock.

At the Distorp site, regional bedrock maps and petrophysical data from SGU indicate that the bedrock is dominated by granitoids, which typically have low magnetic suscepti-

bilities and relatively high thermal conductivities. Within these granitic rocks, occurrences of more mafic gabbroid rock types can occur, which can have higher magnetic susceptibilities and typically have significantly lower thermal conductivities (cf. Figures 1 and 4). Hence, in the case of the Distorp site, the magnetic survey proved to be the most useful ground geophysical tool for pre-investigation. Firstly, it allowed regions with more mafic rocks to be mapped in more detail, as these rocks often exhibit relatively high magnetic susceptibility values. The magnetic data also allowed several local deformation zones to be interpreted based on linear discontinuities in the measurements. Updates to the bedrock geology map for the Distorp site, although based on all the available data from the study, relied heavily on the newly acquired ground magnetic data (Figure 8a).

The VLF-survey gave complimentary information on the occurrence of deformation zones which appear as low resistive features in the data. In the Linköping area, a single potential water-bearing deformation zone was interpreted. Although there is uncertainty in the interpretation of this data, it is beneficial to avoid such potential features when planning an HT-BTES well-cluster. The ground-based geophysical investigations, which required only a fraction of the time and resources required to drill an investigation well, can therefore be considered relatively efficient tools for assessing the lateral anisotropy of the bedrock across the Distorp site. However, it is important to note that interpretation of these ground geophysical data is to some degree subjective, and hence, uncertain. Furthermore, to interpret the ground geophysical data effectively, a good understanding of the petrophysical properties of the rock types in the study area is required. A limitation of ground magnetic and VLF measurements is that they are affected by the presence of infrastructure. Hence, due to the presence of powerlines, it was not possible to acquire VLF data in the entire southern part of the study area. Furthermore, magnetic measurements close to infrastructure or large metallic objects (such as farming machinery or fences) could not be used. Therefore, ground geophysical methods are likely to be most effective as a pre-investigation tool when there is some flexibility in the placement of the HT-BTES system within a larger investigation area with anisotropic bedrock conditions and sparse infrastructure.

Ground gravity measurements were not collected as part of this investigation, due to limitations with resources and equipment availability during the project. However, based on the petrophysical data, there is a clear difference in density values between the mafic and felsic rocks in the study area (Figure 4). Hence, the regions with mafic rocks would likely have generated a series of gravity anomalies which could have been mapped by a grid of gravity measurements across the study area. Therefore, the acquisition of gravity measurements would be recommended for further geophysical investigations at the Distorp site or for pre-site investigations of other HT-BTES projects within similar geological settings.

Outcrop studies have also provided valuable information during the investigations at the Distorp site and have proven to be essential for the interpretation of the ground geophysical data and revision of the bedrock geology map. The use of drone photographs to image and map outcrops proved to be an efficient method for generating a statistical assessment of the primary fracture orientations in the study area, which is valuable data for subsequent modeling work. During the study, lab measurements of thermal conductivity and petrophysical properties, such as density and magnetic susceptibility, have provided highly valuable information which can be useful for calibrating subsequent modeling efforts, as well as interpreting other data collected in the project. A downside of these observations is that measurements are often constrained to specific outcrop locations, which are not evenly distributed across the study area. Hence, this can lead to bias in the subsequent analysis of these data.

The updated geological map for the study area (Figure 8) is assessed to be an improvement from the pre-existing geological map (Figure 1). This is primarily because the more regional map shown in Figure 1 is based on relatively few geological observations and relatively low resolution airborne geophysical measurements. The more detailed map in Figure 8 incorporates and is consistent with additional outcrop observations. Further-

more, some of the geological boundaries have been re-interpreted to be consistent with the detailed ground magnetic data.

However, it is important to note that this geological interpretation could be further improved with additional modeling and analysis of the data. In this project, the results from the different geophysical methods were largely used separately to update the geological map of the study area. This was mainly due to resource constraints during the project. However, in other studies, it has been shown that more accurate and consistent geological interpretations can be achieved if the ground geophysical data is combined, with the available borehole and outcrop data to generate a single 3D geological model [46,47]. In such approaches, it is also possible to process (invert) the data from various geophysical methods together to obtain a more robust result [48,49]. Hence, additional 3D modeling work and joint processing of the data could lead to improvements in the assessment of the site geology and hence, better placement of a potential HT-BTES system.

The use of percussion-drilled investigation wells is not the best way to collect measurements of the subsurface properties. Although data from TRT and DTRT measurement and geophysical wireline logging provide valuable information, there is a problem in correlating the precise rock type to the geophysical and thermal properties. Hence, it is challenging to combine the well results with the ground geophysical measurements. Acquisition of drill core, along with measurements of the susceptibility and analyses of the thermal conductivity coupled to rock type, would greatly enhance the understanding of how the lithological and physical properties of the bedrock are related. Although it is a relatively expensive method, the quality of the information justifies that at least one fully cored borehole is drilled in pre-investigations for larger HT-BTES projects. Wireline logging of the cored borehole could then be used as a reference to interpret log data acquired in additional (relatively cheap) percussion boreholes strategically placed within the site area.

The wireline log data were important, together with the cuttings, to interpret the lithology in the wells. However, they were also used to identify fracturing, water-bearing zones, and assess the orientation of the boreholes. Furthermore, if spectral gamma-ray measurements are used in percussion drilled boreholes, this would enable calculations of heat productivity and more clearly distinguish potassium-poor mafic rock types, such as gabbro, from potassium-rich granitoids.

The geological prerequisites play an important role in the borehole design. Vertical wells are important as the intersection between wells can cause problems when installing the well collector tubing. Strongly deviated wells will also typically not reach the designed depth and bottomhole temperature. A foliated and fractured rock may increase the risk of deviation.

Within the site selection and the BTES design process, the use of conceptual and simulation models is central in assessing the thermal performance and environmental impact of the system. In this context, data collected from extensive field observations provide a useful base for selecting appropriate model parameters, as well as for model validation purposes. In particular, the validity of the common assumptions made in system modeling (e.g., conduction-only heat transfer in homogeneous porous media) can be assessed. Furthermore, it allows for evaluating the applicability of conventional field investigation methods (e.g., TRT) typically employed for collecting data to determine requisite model input parameters.

In this study, the geophysical and geological observations indicate that substantial lateral heterogeneity in the subsurface thermal properties occurs on a scale smaller than that of a typical large-scale BTES facility (Figure 8). It is also the case that a typical-duration TRT only samples a small portion of the storage volume. Given these factors, there is a high probability that a homogeneous model based on TRT data alone, with limited spatial coverage, would not be capable of accurately representing the global characteristics of the large-scale system. The potential limitation of assuming a single TRT-based thermal conductivity estimate to be representative at storage-scale was demonstrated by [15]. Here [15] compared the long-term prediction accuracy of a homogeneous TRT-based

finite element model with that of a vertically layered heterogeneous model with material properties inferred from inverse modeling of long-term soil temperature observational data.

The use of ground geophysical and outcrop studies in the early stage of the pre-investigation process could provide useful information on storage-scale heterogeneity for optimization of subsequent borehole investigations (e.g., DTRT and thermal core analysis, wireline logging, etc.). The combined storage- and borehole-scale data could ultimately be used for parameter estimation, e.g., by geostatistical analysis (see for example [50–52]). Furthermore, the use of hydraulic testing and fracture mapping techniques (e.g., borehole televiewer, outcrop, and core studies) for hydrogeological characterization could provide valuable model input data in the design and environmental assessment processes.

In the final part of this section, the optimal placement of a potential future HT-BTES system at the Distorp site is discussed, considering the available data. The potential HT-BTES in Linköping would involve drilling approximately 1400 wells, with an equidistance of five meters, which would take up an area of approximately 0.04 km² (200 × 200 m). Thus, this would require considerably less space than the entire site area of approximately 2 km², presenting the opportunity to optimize the proposed location of the HT-BTES system. Ideally, such a facility would be located within granitic rocks (with high thermal conductivity) and within a region with relatively few fractures. Therefore, based on the updated bedrock geology map of the study area (based on a range of measurements collected in this study), a location approximately 500 m north of the Distorp Hagen well can be suggested (Figure 8a). The specified area is interpreted to consist of relatively homogeneous granite. In the VLF data, this location lies within a region of relatively high resistivity, which could indicate that it is relatively unfractured. This location is also characterized by relatively low magnetic field values, which likely indicate more granitic rocks. Hence, this area would be a good potential target for further investigation. However, due to uncertainty in the bedrock geology map and the potential for heterogeneity at depth, additional investigation wells at this location are required to further assess the suitability of this location.

6. Conclusions

In this study, a multidisciplinary approach has been applied to further assess the anisotropic crystalline bedrock at the Distorp site at Linköping as a potential storage medium for an HT-BTES system. The investigations conducted include surface-based geophysical measurements, outcrop observations, and lab measurements of samples. Furthermore, detailed investigations within two boreholes inside the study area were conducted, including geophysical well logging, DTRT, flow logs, and pump tests. This multidisciplinary approach has proved invaluable in characterizing the anisotropic bedrock and its anticipated thermal properties across the approximately 2 km² study area. Based on these results, a subregion of the study area is highlighted for further investigation as a potential site for an HT-BTES system. As well as highlighting the strengths of a multidisciplinary approach, the suitability of the different methods utilized in this study for BTES appraisal work are discussed with regards to their strengths and limitations.

Traditionally, pre-site investigations for BTES systems only involve observations in one or several investigation wells. However, when considering large scale HT-BTES systems that utilize anisotropic crystalline bedrock as a storage medium, a pre-investigation strategy based only on well observations is likely to be inadequate. In such situations, leverage of a range of methods that can adequately characterize the variability of the bedrock properties is important for the successful assessment of performance and design of a BTES facility. Hence, this multidisciplinary study has shown that re-evaluating the way pre-investigations are typically performed is necessary when it comes to the optimization of large HT-BTES.

Supplementary Materials: The following are available online at <https://www.mdpi.com/article/10.3390/en14144379/s1>, Figure S1: Distorp Hagen 240 m Acoustic televiewer, Figure S2: Distorp Hagen 300 m Acoustic televiewer, Table S1: Supplementary information on the equipment used for the various methods, Table S2: Mean, minimum and maximum values for each of the lab based TCS measurements performed on samples from the Distorp area, Table S3: Calculated thermal conductivity based on the modal analyses of the mineral composition on rock samples of various typical rock types within five-kilometer radius from the Distorp site, Table S4: Individual measurements from the gamma spectrometer for the different rock types in the Distorp area, Spreadsheet S1: DTRT data Distorp Åkern.

Author Contributions: Conceptualization, M.E., J.A., M.H. and D.S.; methodology, M.E., M.H. and D.S.; software, D.S. and M.H.; validation, M.H., J.A. and D.S.; formal analysis, M.H., D.S. and M.E.; investigation, D.S., M.H. and M.E.; resources, J.A. and M.E.; data curation, M.H. and D.S.; writing—original draft preparation, M.H., M.E. and D.S.; writing—review and editing, M.H., M.E., D.S. and J.A.; visualization, D.S., M.H. and M.E.; supervision, J.A. and M.E.; project administration, M.E. and J.A.; funding acquisition, J.A. and M.E. All authors have read and agreed to the published version of the manuscript.

Funding: This research was funded by the European Union’s Horizon 2020 research and innovation program under grant agreement No. 731166 and under the terms of the GeoERA program—ERANET Cofund Action, and by Energiforsk and the Norwegian University of Science and Technology (NTNU).

Institutional Review Board Statement: Not applicable.

Informed Consent Statement: Not applicable.

Data Availability Statement: The regional geological and geophysical measurements as well as the newly acquired measurements over the study area are publicly available via the Swedish Geological survey’s customer service (<https://www.sgu.se/en/products/>, accessed on 12 July 2021).

Acknowledgments: We especially want to thank Tekniska Verken in Linköping AB and Henrik Lindståhl for the support and letting us use information from and access to the Distorp site as a pilot site within the GeoERA MUSE project.

Conflicts of Interest: The authors declare no conflict of interest. The funders had no role in the design of the study; in the collection, analyses, or interpretation of data; in the writing of the manuscript, or in the decision to publish the results.

References

1. Forman, C.; Muritala, I.K.; Pardemann, R.; Meyer, B. Estimating the global waste heat potential. *Renew. Sustain. Energy Rev.* **2016**, *57*, 1568–1579. [[CrossRef](#)]
2. Gehlin, S. 11-Borehole thermal energy storage. In *Advances in Ground-Source Heat Pump Systems*; Rees, S.J., Ed.; Woodhead Publishing: Cambridge, UK, 2016; pp. 295–327. ISBN 978-0-08-100311-4.
3. Malmberg, M. Transient Modeling of a High Temperature Borehole Thermal Energy Storage Coupled with a Combined Heat and Power Plant. Master’s Thesis, Royal Institute of Technology, Stockholm, Sweden, 2017.
4. Linköping Climate: Average Temperature, Weather by Month, Linköping Weather Averages-Climate-Data.Org. Available online: <https://en.climate-data.org/europa/sverige/oestergoetlands-laen/linkoeeping-80/> (accessed on 14 June 2021).
5. Statistics | Eurostat. Available online: https://ec.europa.eu/eurostat/databrowser/view/nrg_chddr2_a/default/table?lang=en (accessed on 15 June 2021).
6. Lejonpannan. Available online: <https://www.tekniskaverken.se/om-oss/anlaggningar/kraftvarmeverk/lejonpannan/?login=reset> (accessed on 15 June 2021).
7. Malmberg, M.; Mazzotti, W.; Acuña, J.; Lindståhl, H.; Lazzarotto, A. High temperature borehole thermal energy storage—A case study. In Proceedings of the IGSHPA Research Track, Stockholm, Sweden, 18–19 September 2018; pp. 380–388.
8. Acuña, J.; Lazzarotto, A.; Garcia, J.; Mazzotti-Pallard, W.; Topel, M.; Hesselbrandt, M.; Malmberg, M.; Abuasbeh, M. *Tools For Design of High Temperature Borehole Storage in District Heating Production*; Termiska Energilager; Energiforsk: Stockholm, Sweden, 2021; ISBN 978-91-7673-770-5.
9. Catolico, N.; Ge, S.; McCartney, J.S. Numerical Modeling of a Soil—Borehole Thermal Energy Storage System. *Vadose Zone J.* **2016**, *15*, 1–17. [[CrossRef](#)]
10. Welsch, B.; Rühaak, W.; Schulte, D.O.; Bär, K.; Sass, I. Characteristics of medium deep borehole thermal energy storage. *Int. J. Energy Res.* **2016**, *40*, 1855–1868. [[CrossRef](#)]

11. Nguyen, A.; Pasquier, P.; Marcotte, D. Borehole thermal energy storage systems under the influence of groundwater flow and time-varying surface temperature. *Geothermics* **2017**, *66*, 110–118. [CrossRef]
12. Schincariol, R.A.; Raymond, J. Borehole Heat Exchangers—Addressing the Application Gap with Groundwater Science. *Ground Water* **2021**. [CrossRef] [PubMed]
13. Dehkordi, S.; Schincariol, R. Guidelines and the design approach for vertical geothermal heat pump systems: Current status and perspective. *Can. Geotech. J.* **2014**, *51*, 647–662. [CrossRef]
14. Spitler, J.D.; Bernier, M. 2—Vertical borehole ground heat exchanger design methods. In *Advances in Ground-Source Heat Pump Systems*; Rees, S.J., Ed.; Woodhead Publishing: Sawston, UK, 2016; pp. 29–61. ISBN 978-0-08-100311-4.
15. Tordrup, K.W.; Poulsen, S.; Bjørn, H. An improved method for upscaling borehole thermal energy storage using inverse finite element modelling. *Renew. Energy* **2017**, *105*, 13–21. [CrossRef]
16. Banks, D. A review of the importance of regional groundwater advection for ground heat exchange. *Environ. Earth Sci.* **2015**, *73*, 2555–2565. [CrossRef]
17. Stephens, M.B.; Jansson, N.F. Chapter 6 Paleoproterozoic (1.9–1.8 Ga) syn-orogenic magmatism, sedimentation and mineralization in the Bergslagen lithotectonic unit, Svecokarelian orogen. *Geol. Soc. London, Memoirs* **2020**, *50*, 155–206. [CrossRef]
18. Claeson, D.; Antal Lundin, I.; Sukotjo, S. *K 438 Beskrivning till Berggrundskartan Delar Av Mjölby, Linköpings Och Norrköpings Kommuner*; Sveriges Geologiska Undersökning: Uppsala, Sweden, 2013; ISBN 978-91-7403-223-9.
19. Gorbatshev, R.; Fromm, E.; Kjellström, G. *Af 107 Description to the Map of Solid Rocks Linköping NO.*; Geological Survey of Sweden: Stockholm, Sweden, 1976; ISBN 91-7158-093-X.
20. Wickström, L.M.; Stephens, M.B. Tonian–Cryogenian rifting and Cambrian–Early Devonian platformal to foreland basin development outside the Caledonide orogen. In *Sweden: Lithotectonic Framework, Tectonic Evolution and Mineral Resources*; Stephens, M.B., Bergman Weihed, J., Eds.; Geological Society of London: London, UK, 2020; Volume 50, pp. 451–477. ISBN 978-1-78620-460-8.
21. Brunnar. Available online: <http://resource.sgu.se/service/wms/130/brunnar> (accessed on 15 June 2021).
22. Acuña, J.; Stokuca, M.; Mazzotti, W.; Munter, E. Förundersökningar För Högtemperaturlager. Provbörning Och Responsmätning Vid NetonNet, Dikestriangeln, Distorp Åker Och Distorp Hagen (in Swedish). Unpublished.
23. Hesselbrandt, M.; Acuña, J.; Funehag, J. *Impermeable Boreholes for High Temperature Thermal Energy Storage*; Termiska Energilager; Energiforsk: Stockholm, Sweden, 2020; ISBN 978-91-7673-666-1.
24. Kearey, P.; Brooks, M.; Hill, I. *An Introduction to Geophysical Exploration*, 3rd ed.; Blackwell Science: Malden, MA, USA, 2002; ISBN 0-632-04929-4.
25. Geofysiska Markmätningar, Tyngdkraft. Available online: <http://resource.sgu.se/service/wms/130/markgeofysik-tyngdkraft> (accessed on 15 June 2021).
26. Popov, Y.A.; Berezin, V.; Semionov, V.G.; Korosteliov, V.M. Complex Detailed Investigations of the Thermal Properties of Rocks on the Basis of a Moving Point Source. *Izv. Earth Phys.* **1985**, *21*, 64–70.
27. Liu, H. *Principles and Applications of Well Logging*, 2nd ed.; Springer Geophysics; Springer: Berlin/Heidelberg, Germany, 2017; ISBN 978-3-662-54976-6.
28. Geological Log Analysis. Available online: http://www.kgs.ku.edu/Publications/Bulletins/LA/09_igneous.html (accessed on 15 June 2021).
29. Bücker, C.; Rybach, L. A simple method to determine heat production from gamma-ray logs. *Mar. Pet. Geol.* **1996**, *13*, 373–375. [CrossRef]
30. Loke, M.H. Tutorial: 2-D and 3-D Electrical Imaging Surveys. Available online: <https://www.geotomosoft.com/coursenotes.zip> (accessed on 19 July 2021).
31. Skarphagen, H.; Banks, D.; Frengstad, B.S.; Gether, H. Design Considerations for Borehole Thermal Energy Storage (BTES): A Review with Emphasis on Convective Heat Transfer. *Geofluids* **2019**, *2019*, 1–26. [CrossRef]
32. Spitler, J.D.; Gehlin, S.E. Thermal response testing for ground source heat pump systems—An historical review. *Renew. Sustain. Energy Rev.* **2015**, *50*, 1125–1137. [CrossRef]
33. Carslaw, H.S.; Jaeger, J.C. *Conduction of Heat in Solids*; Oxford University Press: Oxford, UK, 1959; ISBN 978-0-19-853303-0.
34. Simon, N.; Bour, O.; Lavenant, N.; Porel, G.; Nauleau, B.; Pouladi, B.; Longuevergne, L. A Comparison of Different Methods to Estimate the Effective Spatial Resolution of FO-DTS Measurements Achieved during Sandbox Experiments. *Sensors* **2020**, *20*, 570. [CrossRef] [PubMed]
35. Aranzabal, N.; Martos, J.; Stokuca, M.; Pallard, W.M.; Acuña, J.; Soret, J.; Blum, P. Novel instruments and methods to estimate depth-specific thermal properties in borehole heat exchangers. *Geothermics* **2020**, *86*, 101813. [CrossRef]
36. Acuña, J. Distributed Thermal Response Tests—New Insights on U-Pipe and Coaxial Heat Exchangers in Groundwater-Filled Boreholes. Ph.D. Thesis, Royal Institute of Technology, Stockholm, Sweden, 2013.
37. Moye, D.G. Diamond Drilling for Foundation Exploration. *Civ. Eng. Trans.* **1967**, *CE9*, 95–100.
38. Andolfsson, T. Analyses of Thermal Conductivity from Mineral Composition and Analyses by Use of Thermal Conductivity Scanner : A Study of Thermal Properties of Scania Rock Types. Master’s Thesis, Lund University, Lund, Sweden, 2013.
39. Witte, H.J.L. Error Analysis of Thermal Response Tests. *Appl. Energy* **2013**, *109*, 302–311. [CrossRef]
40. Gustafsson, A.-M. Thermal Response Tests: Influence of Convective Flow in Groundwater Filled Borehole Heat Exchanger. Ph.D. Thesis, Luleå Tekniska Universitet, Luleå, Sweden, 2010.

41. Dershowitz, W.S.; Herda, H.H. Interpretation of Fracture Spacing and Intensity. In Proceedings of the The 33th U.S. Symposium on Rock Mechanics (USRMS), Santa Fe, NM, USA, 3–5 June 1992; American Rock Mechanics Association: Santa Fe, NM, USA, 1992.
42. Mäkelä, J. Drilled Well Yield and Hydraulic Properties in the Precambrian Crystalline Bedrock of Central Finland. Ph.D. Thesis, University of Turku, Turku, Finland, 2012.
43. Cheema, T. Depth dependent hydraulic conductivity in fractured sedimentary rocks—a geomechanical approach. *Arab. J. Geosci.* **2015**, *8*, 6267–6278. [[CrossRef](#)]
44. Bense, V.F.; Read, T.; Bour, O.; Le Borgne, T.; Coleman, T.; Krause, S.; Chalari, A.; Mondanos, M.; Ciocca, F.; Selker, J.S. Distributed Temperature Sensing as a downhole tool in hydrogeology. *Water Resour. Res.* **2016**, *52*, 9259–9273. [[CrossRef](#)]
45. Bakx, W.; Doornenbal, P.J.; van Weesep, R.J.; Bense, V.F.; Oude Essink, G.H.P.; Bierkens, M.F.P. Determining the Relation between Groundwater Flow Velocities and Measured Temperature Differences Using Active Heating-Distributed Temperature Sensing. *Water* **2019**, *11*, 1619. [[CrossRef](#)]
46. Finn, C.A.; Bedrosian, P.; Cole, J.C.; Khoza, T.D.; Webb, S.J. Mapping the 3D extent of the Northern Lobe of the Bushveld layered mafic intrusion from geophysical data. *Precambrian Res.* **2015**, *268*, 279–294. [[CrossRef](#)]
47. Claeson, D.; Sopher, D. *Investigation of Layered Gabbroic Intrusions, Bergslagen*; Geological Survey of Sweden: Uppsala, Sweden, 2021.
48. Gallardo-Delgado, L.A.; Pérez-Flores, M.A.; Gómez-Treviño, E. A versatile algorithm for joint 3D inversion of gravity and magnetic data. *Geophysics* **2003**, *68*, 949–959. [[CrossRef](#)]
49. Pilkington, M. Joint inversion of gravity and magnetic data for two-layer models. *Geophysics* **2006**, *71*, L35–L42. [[CrossRef](#)]
50. Focaccia, S. Characterization of Geothermal Reservoirs’ Parameters by Inverse Problem Resolution and Geostatistical Simulations. Ph.D. Thesis, Università di Bologna, Bologna, Italy, 2012.
51. Rühaak, W.; Guadagnini, A.; Geiger, S.; Bär, K.; Gu, Y.; Aretz, A.; Homuth, S.; Sass, I. Upscaling thermal conductivities of sedimentary formations for geothermal exploration. *Geothermics* **2015**, *58*, 49–61. [[CrossRef](#)]
52. Linde, N.; Chen, J.; Kowalsky, M.B.; Hubbard, S. Hydrogeophysical Parameter Estimation Approaches for Field Scale Characterization. In *Applied Hydrogeophysics*; Vereecken, H., Binley, A., Cassiani, G., Revil, A., Titov, K., Eds.; NATO Science Series; Springer: Dordrecht, The Netherlands, 2006; Volume 71, pp. 9–44. ISBN 978-1-4020-4912-5.